Prebiotic route to pyrimidine nucleotides

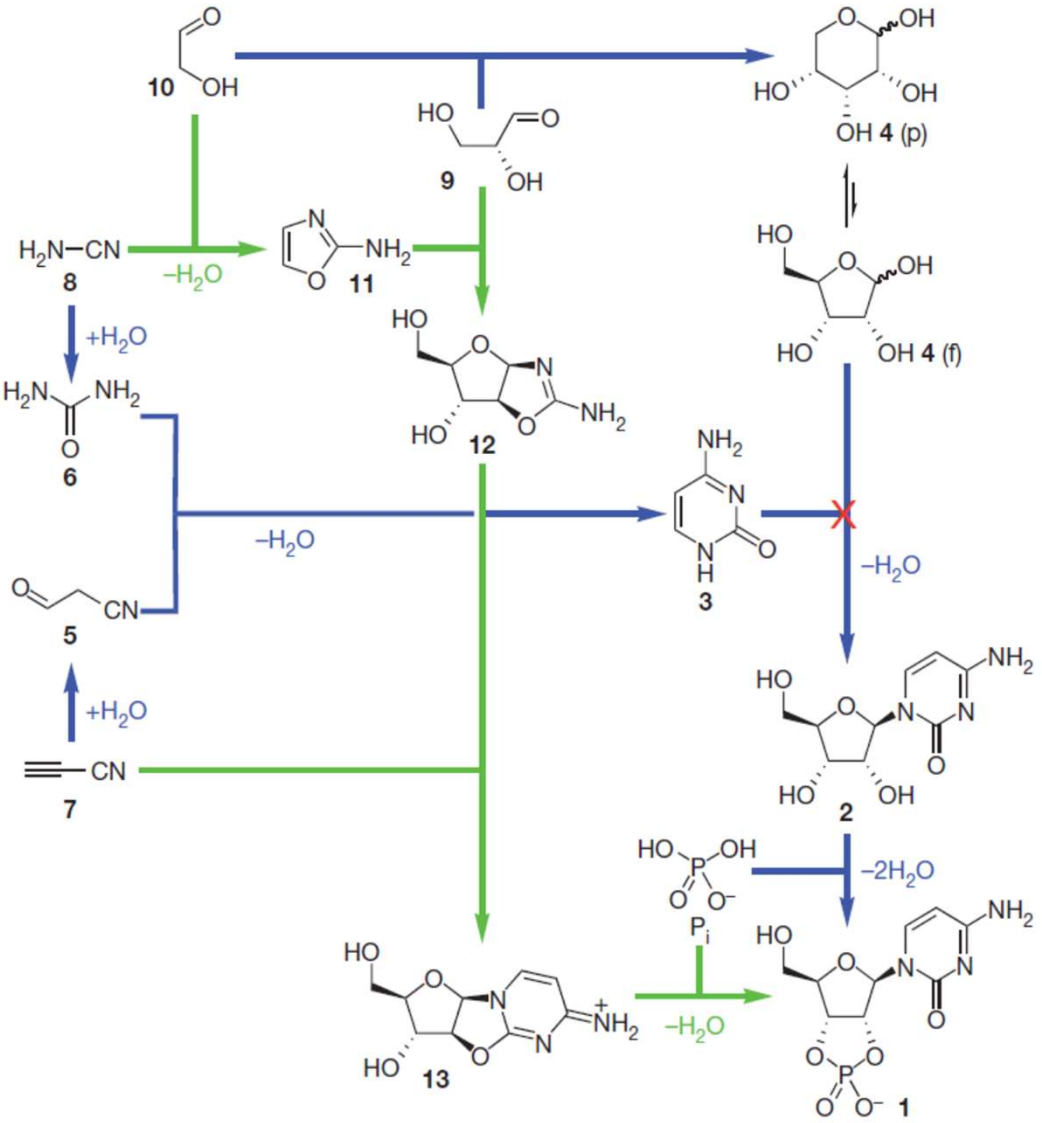

Prof. John Sutherland
Laboratory of Chemical Biology
Cambridge, UK

Dr. Matthew Powner
University College London, UK

The origin of small reactive intermediates

Thermal decomposition of cyanoferrates (volcanic):

$(Na,K)_4[Fe(CN)_6] \xrightarrow{700^oC} 4(\mathbf{Na/K})\mathbf{CN} + Fe(CN)_2$

$3Fe(CN)_2 \xrightarrow{700^oC} Fe_3C + 5C + 3N_2$

$Fe(CN)_2 \xrightarrow{700^oC} Fe + 2C + N_2$

$Ca_2[Fe(CN)_6] \xrightarrow{660^oC} 2Ca(CN)_2 + Fe(CN)_2$

$Ca(CN)_2 \xrightarrow{660^oC} \mathbf{CaNCN} + C \underset{}{\overset{1000^oC}{\rightleftharpoons}} \mathbf{CaC_2} + N_2$

$Mg_2[Fe(CN)_6] \xrightarrow{315^oC} 2Mg(CN)_2 + Fe(CN)_2$

$Mg(CN)_2 \xrightarrow{395^oC} MgCN_2 + C$

$3MgCN_2 \xrightarrow{420^oC} \mathbf{Mg_3N_2} + 3C + 2N_2$

$Cu_2S + H_2O + 6CN^- \rightarrow 2[Cu(CN)_3]^{2-} + HS^- + OH^-$

cyanocuprates and HS^- are delivered by this process

Photoredox cycle based on cyanocuprates may convert HCN into cyanogen

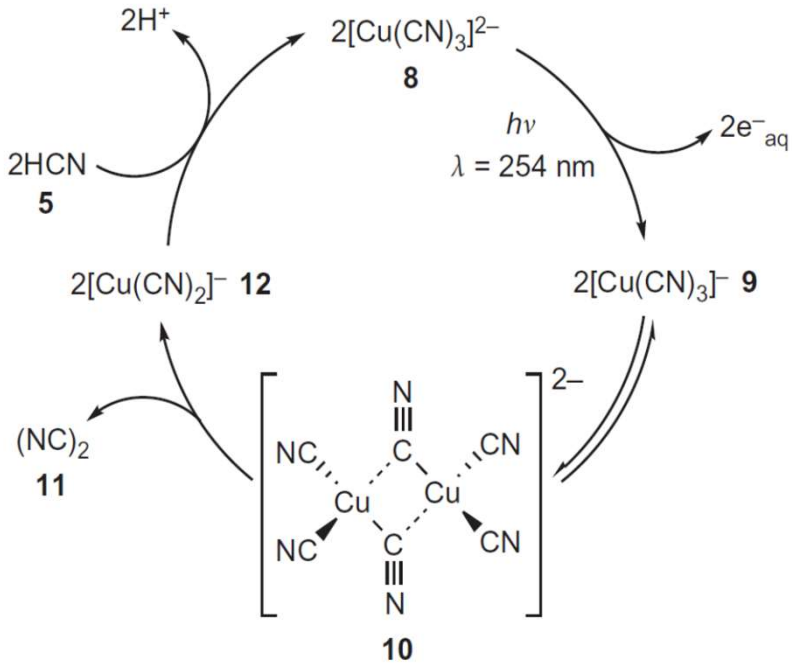

Action of water (bufferred to neutral or slightly acidic) on that mixture produced concentrated HCN solution + cyanamide (from CaNCN) + acetylene (from CaC_2) + ammonia (from Mg_3N_2)

Cyanosulfidic chemistry for the Kiliani-Fischer homologation

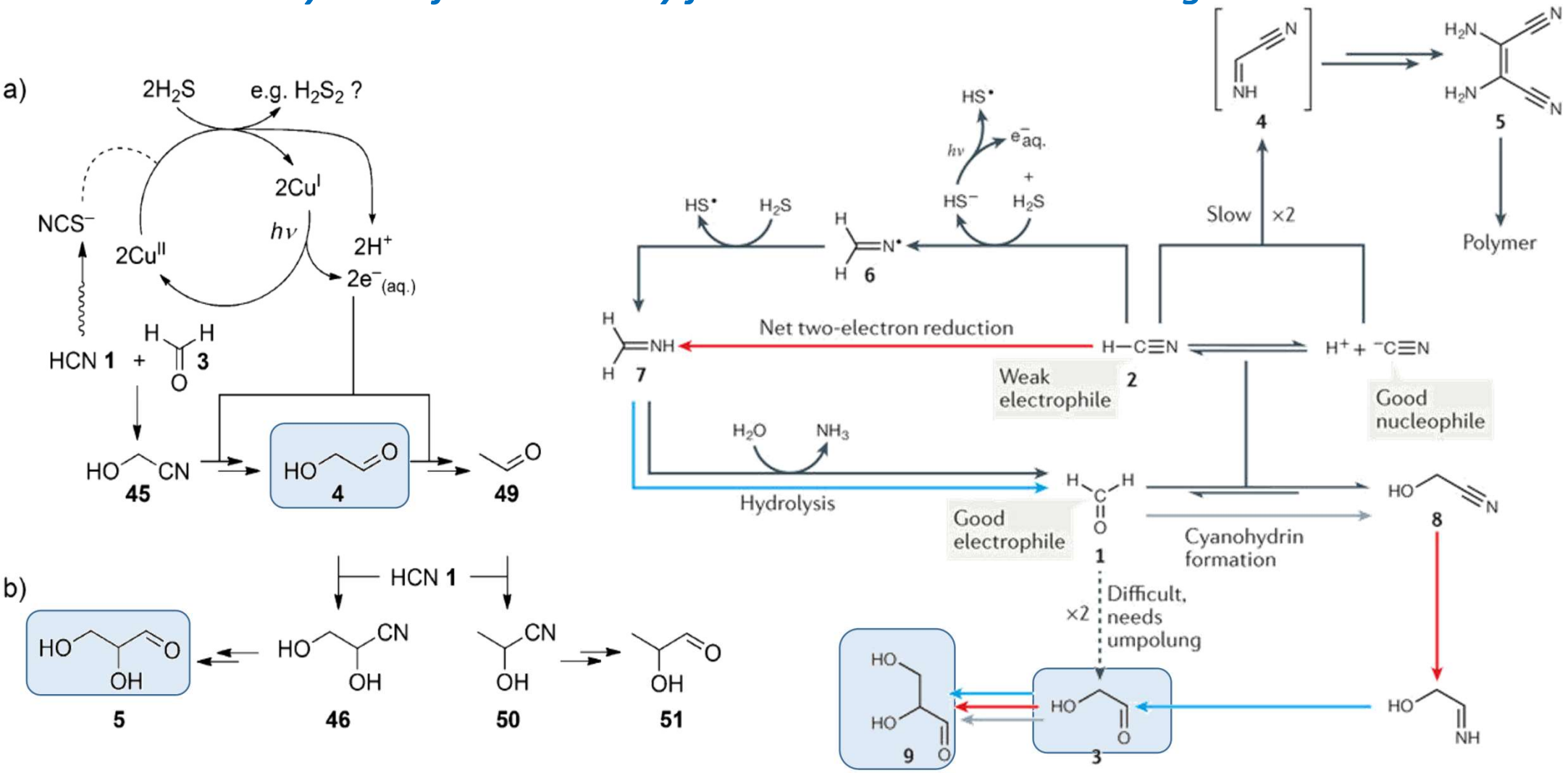

J. Sutherland, *Nature Reviews Chemistry* **2017**, *1*, Article 0012, doi:10.1038/s41570-016-0012

Nature Reviews | Chemistry

Cyanosulfidic chemistry

First signs of a linkage between all subsystems through cyanosulfidic chemistry.

glyceraldehyde **5** is a precursor of pyrimidine nucleotides (**RNA**), Upon isomerization to **53** and reduction to glycerol **54**, it can be phosphorylated to yield phospho**lipids** (from **56** and **57**)...

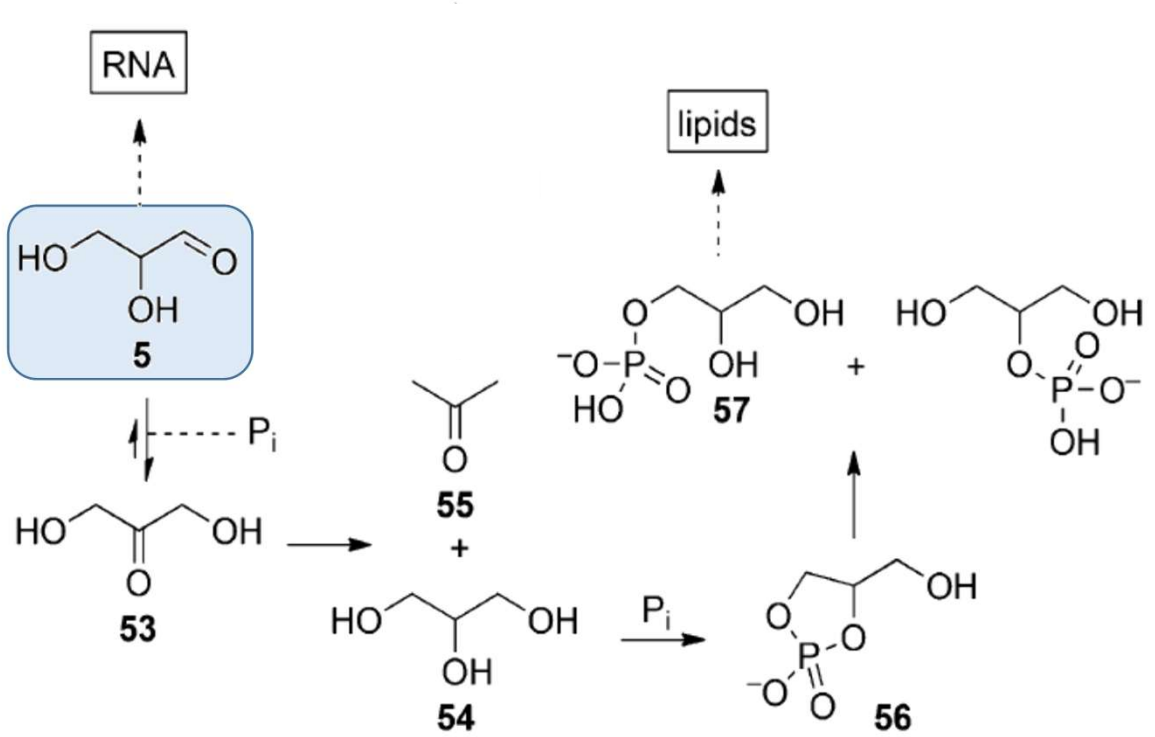

J. D. Sutherland, *et al. Nature Chem.* **2015**, *7*, 301-307

Lipids

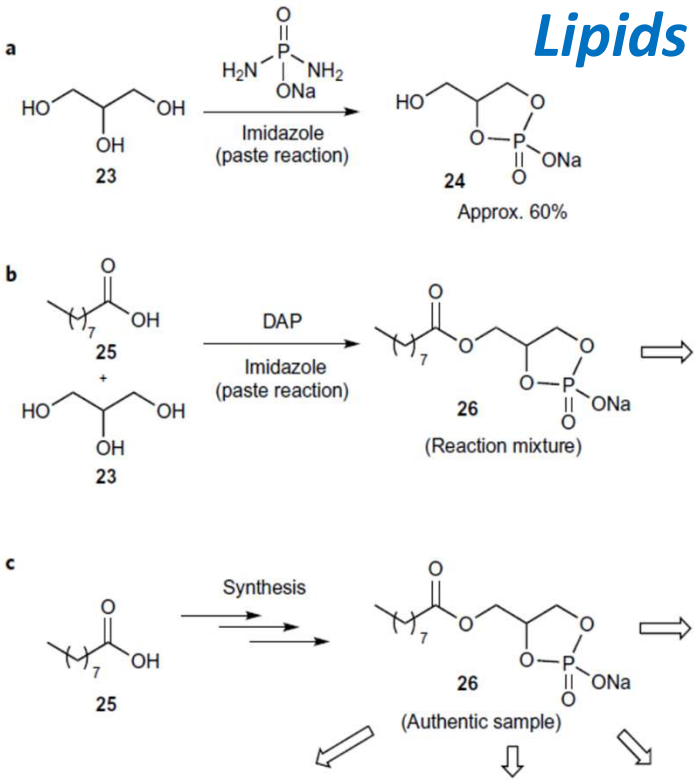

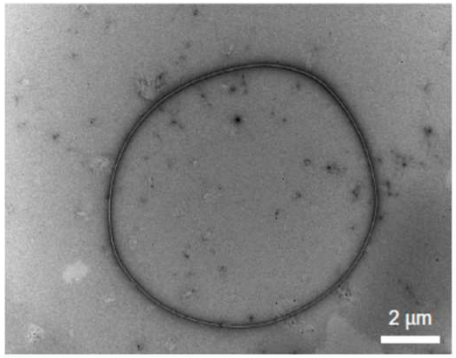

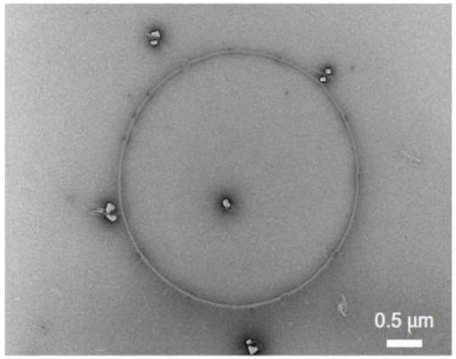

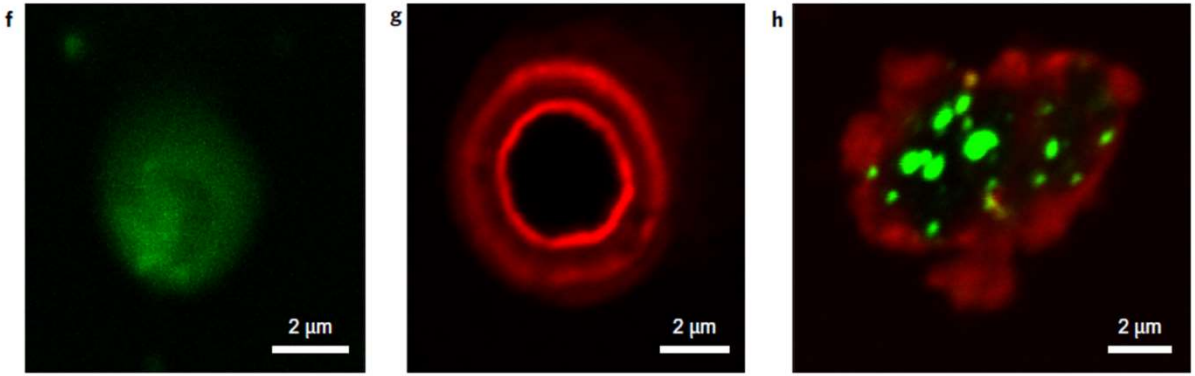

d, TEM image of a sample (15 mg in 1 ml water) from the crude reaction in b, showing the formation of vesicle-like structures with a diameter of ~9.2 µm.

e, TEM image of a sample (1 mg in 1 ml water) of authentic phospholipid 26 from Fig. 2c showing the formation of vesicle-like structures with a diameter of ~3.5 µm.

f–h, Confocal laser scanning microscopy fluorescence images of vesicles prepared with authentic phospholipid **26** (1 mg in 0.1 ml water) with dye encapsulation.

- In **f**, green fluorescence indicates hydrophilic pyranine dye encapsulated within the cavity of the liposome.
- In **g**, red fluorescence indicates rhodamine B dye labelling the bilayer phospholipid membrane of the liposome.
- In **h**, a fluorescence merged image is shown of a phospholipid vesicle prepared with both rhodamine B dye and pyranine dye.

Cyanosulfidic chemistry

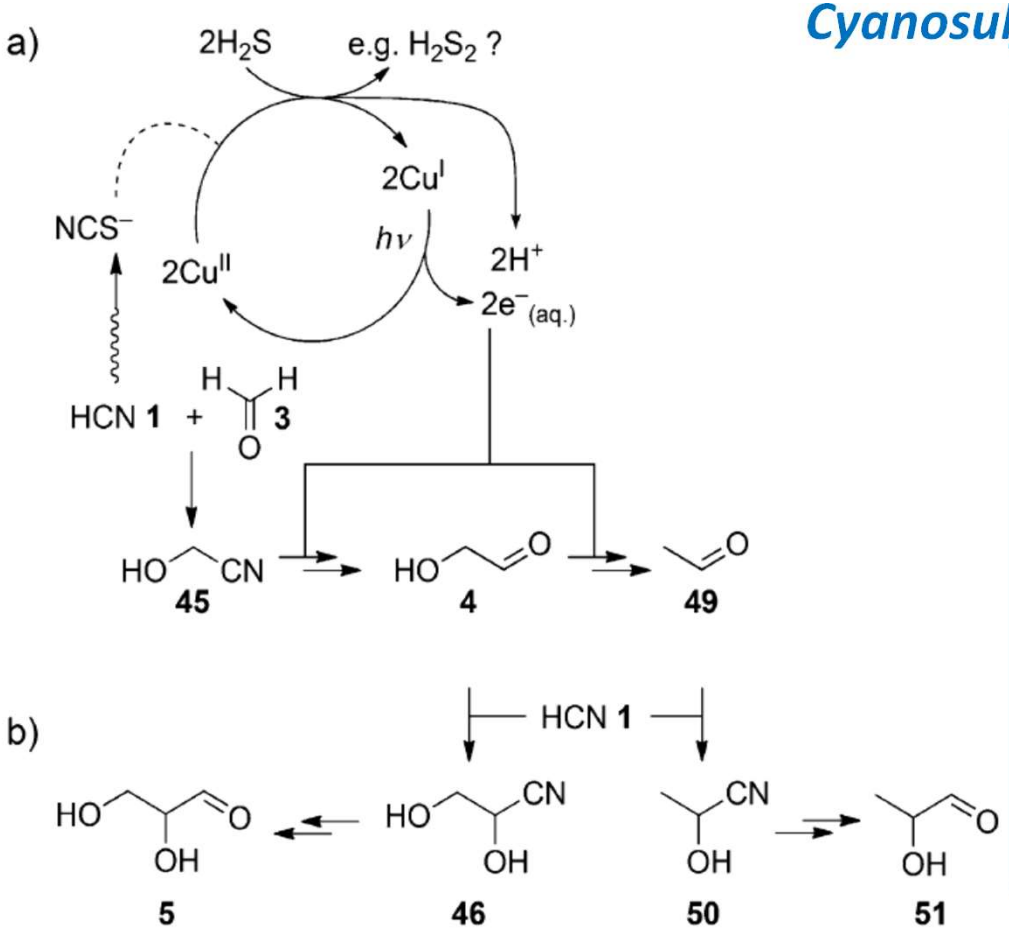

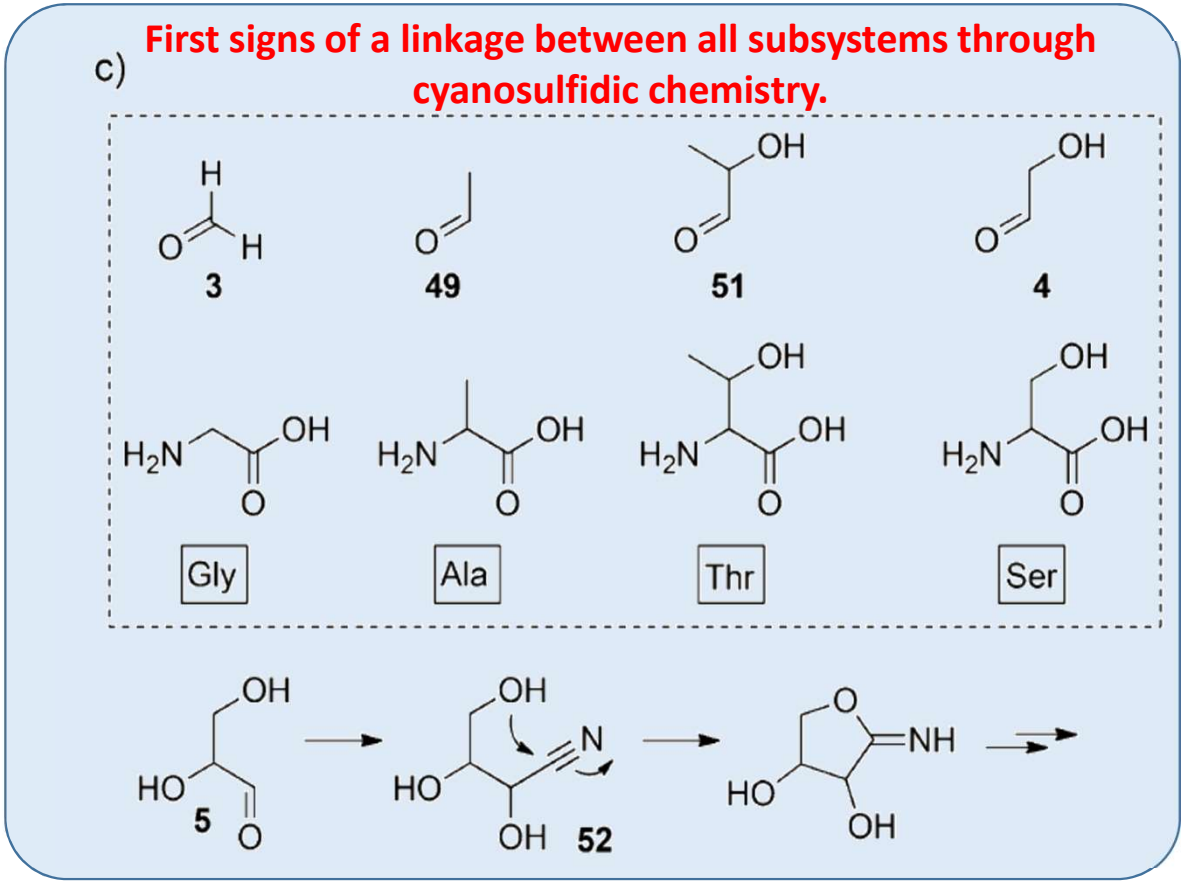

Photoredox systems chemistry with hydrosulfide as the stoichiometric reductant. a) (Over-)reduction of glycolonitrile **45** to glycolaldehyde **4** (and acetaldehyde **49**), b) reductive homologation of **4** (and **49**) to **5** (and **51**), c) most of the aldehydes produced by this chemistry as Strecker amino acid precursors (boxed) and the self-destruction (as regards potential Strecker chemistry) of the cyanohydrin **52**.

J. D. Sutherland, *et al. Nature Chem.* **2015**, *7*, 301-307

Cyanosulfidic chemistry

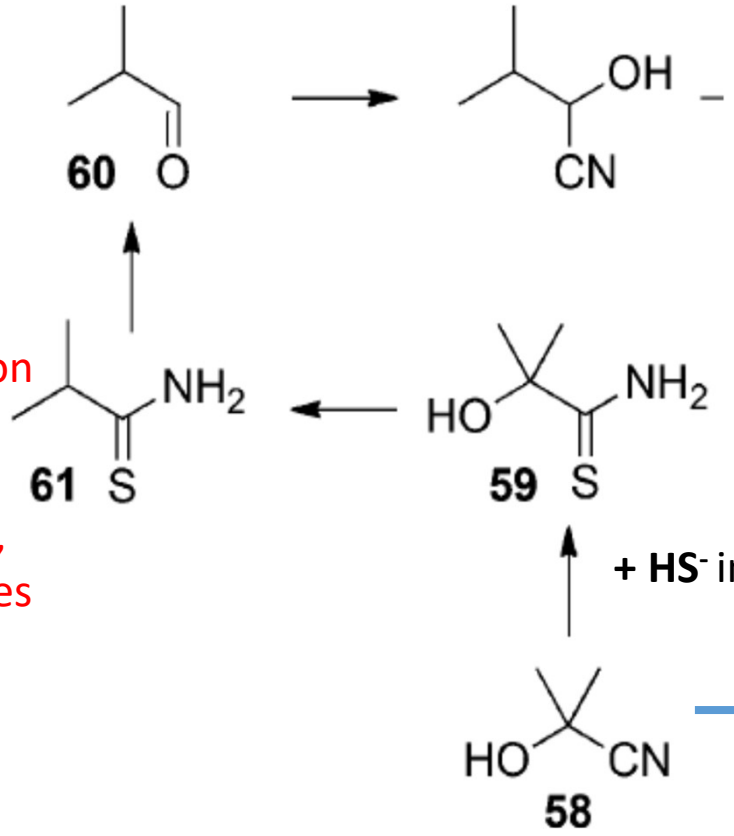

Cyanohydrins undergo photoreduction to α-hydroxyaldehydes. α-hydroxythioamides first undergo photodeoxygenation to thioamides, and then photoreduction to aldehydes

Not reduced under applied conditions

J. D. Sutherland, *et al. Nature Chem.* **2015**, *7*, 301-307

Cyanosulfidic chemistry

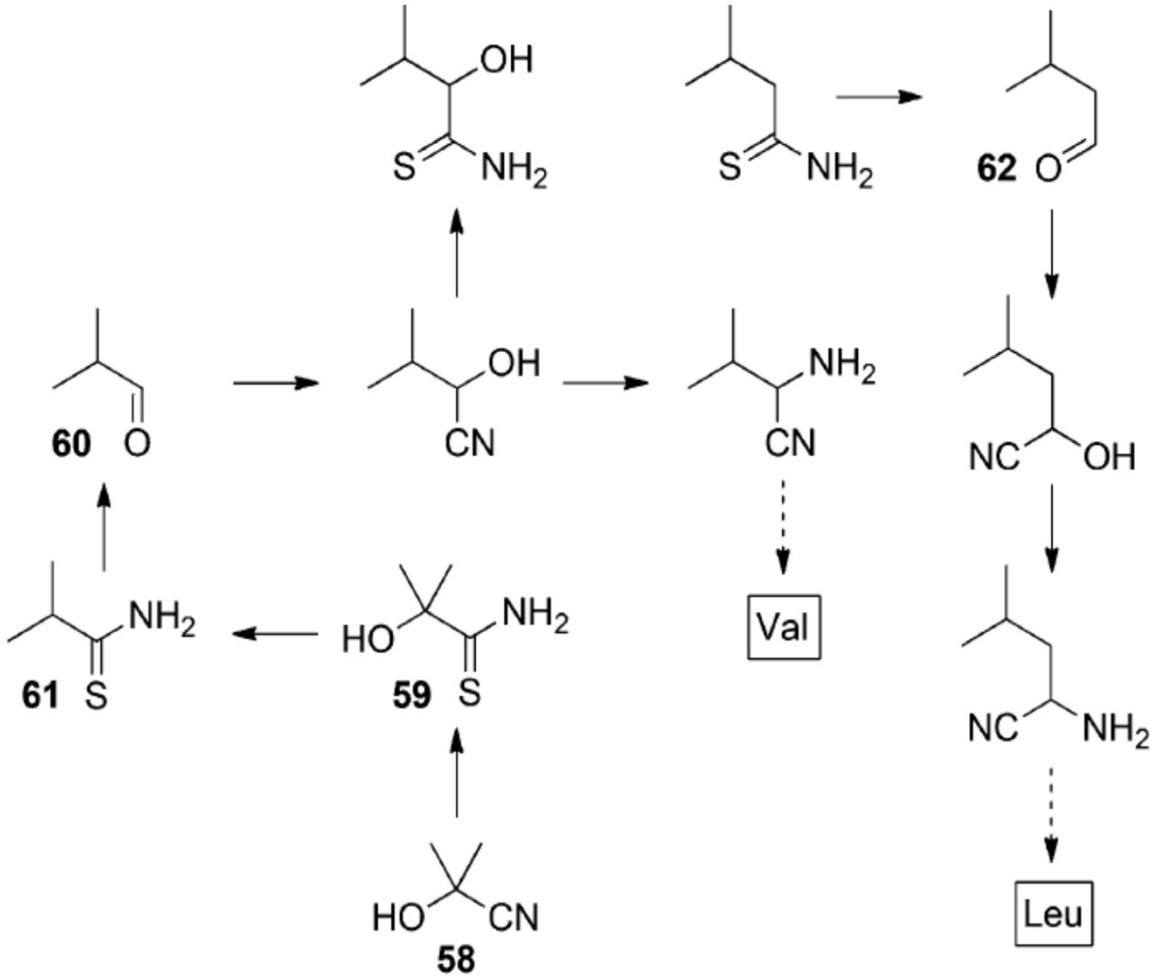

J. D. Sutherland, *et al. Nature Chem.* **2015**, *7*, 301-307

Cyanosulfidic chemistry

First signs of a linkage between all subsystems through cyanosulfidic chemistry.

glyceraldehyde **5** is a precursor of pyrimidine nucleotides (**RNA**), Upon isomerization to **53** and reduction to glycerol **54**, it can be phosphorylated to yield phospho**lipids** (from **56** and **57**)...

The side product – acetone **55** – seems to be meaningful in the potentially prebiotic route for branched **aminoacids** Val and Leu

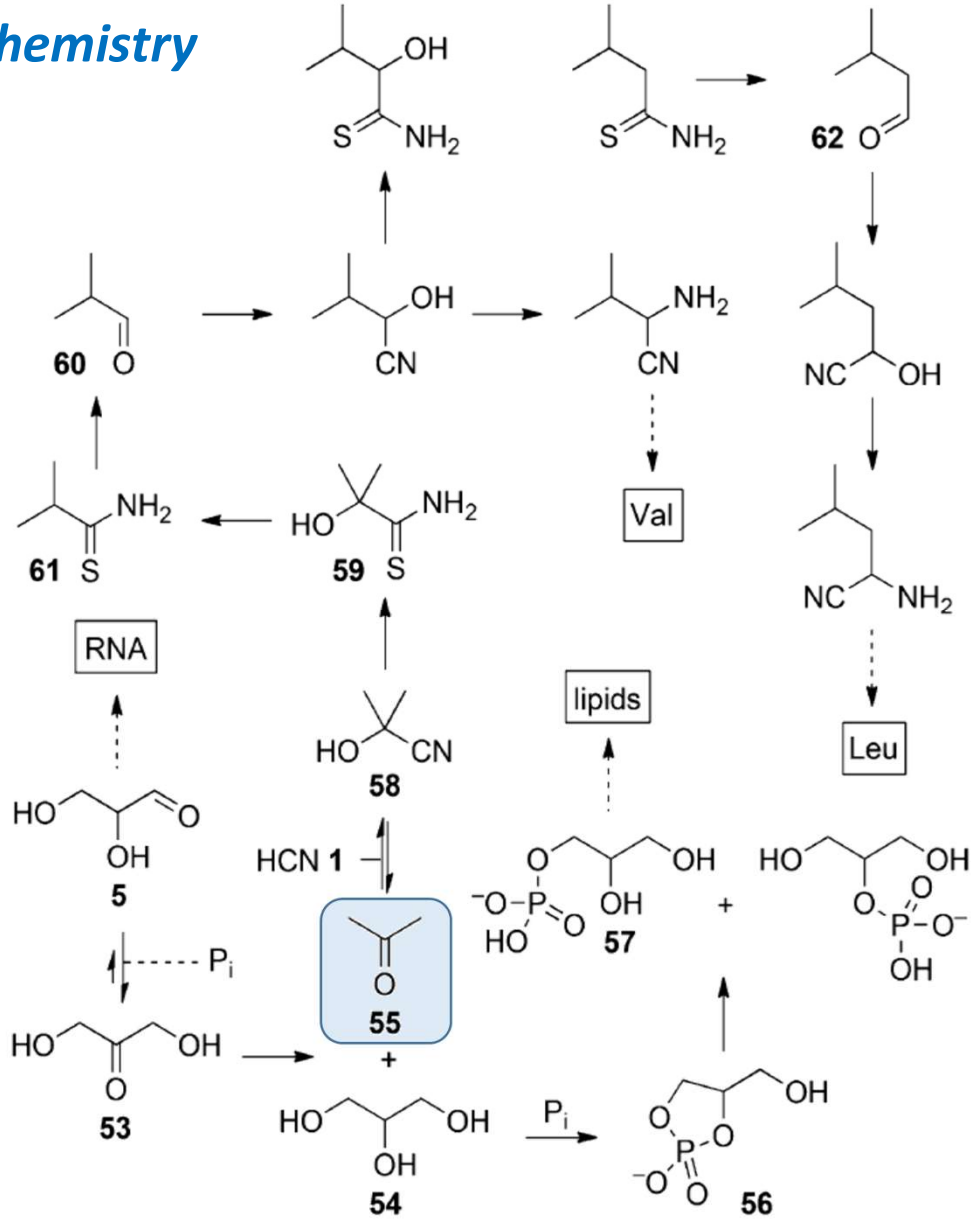

J. D. Sutherland, *et al. Nature Chem.* **2015**, *7*, 301-307

Cyanosulfidic chemistry

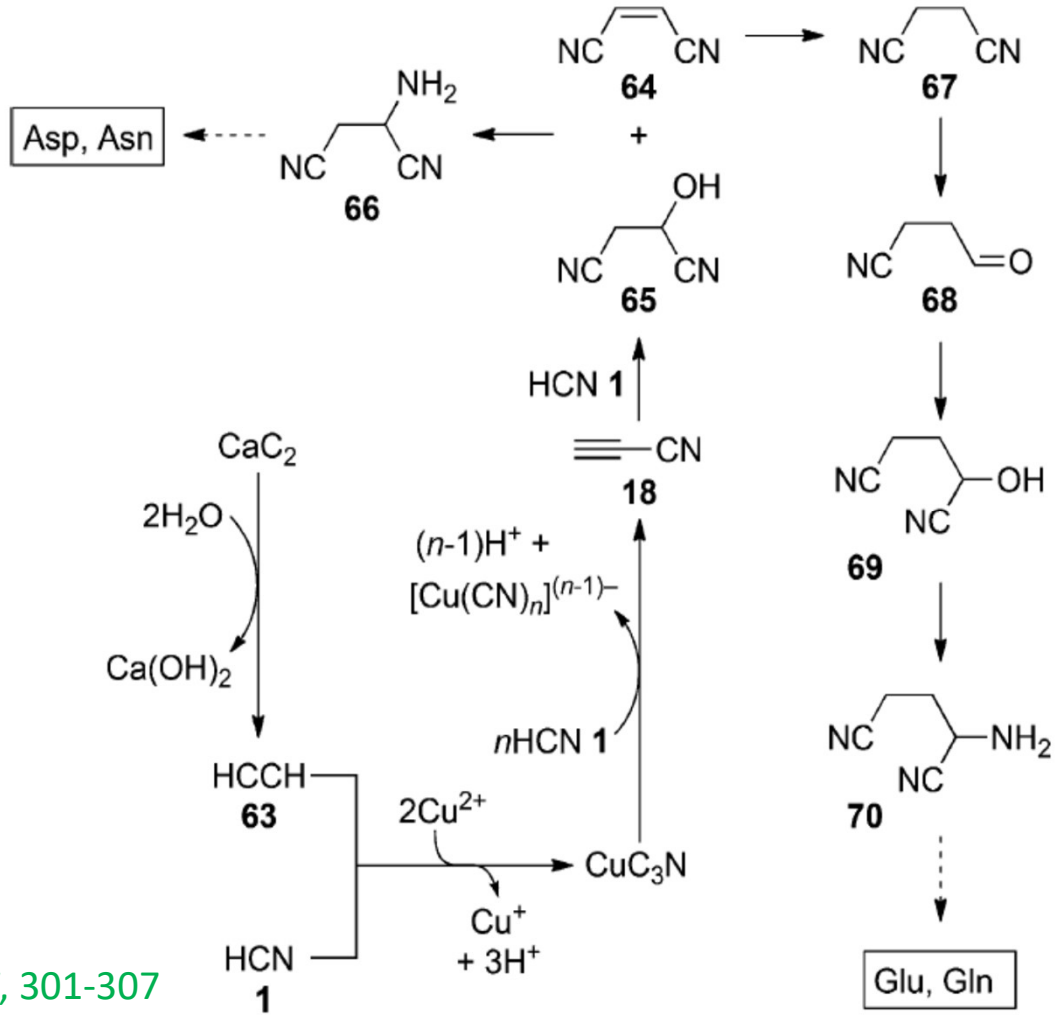

J. D. Sutherland, *et al. Nature Chem.* **2015**, *7*, 301-307

Synthesis of cyanoacetylene **18** and reactions leading to amino acid precursors of Asp/Asn and Glu/Gln.

Cyanosulfidic chemistry

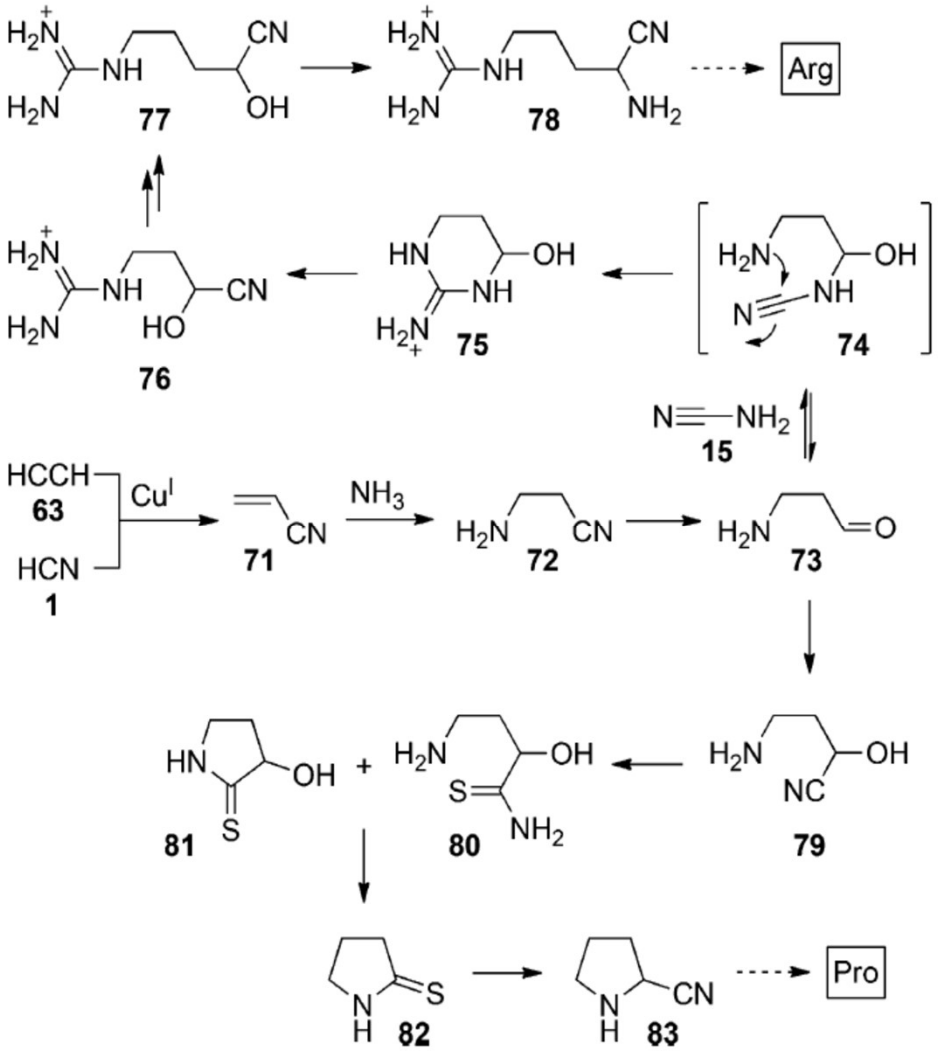

Synthesis of acrylonitrile **71** and reactions leading to amino acid precursors therefrom.

Cyanosulfidic chemistry

Chemistry in a post-meteoritic-impact scenario.
A series of post-impact environmental events are shown along with the chemistry (boxed) proposed to occur as a consequence of these events.

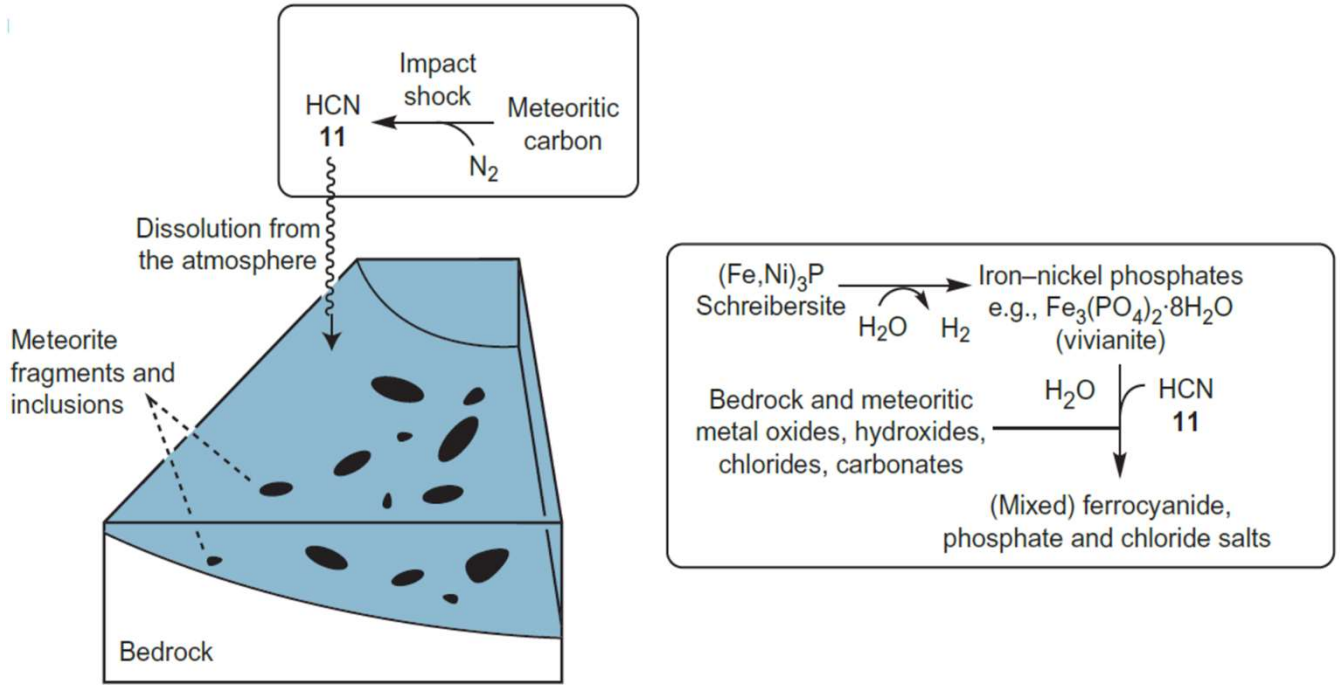

Dissolution of atmospherically produced hydrogen cyanide results in the conversion of vivianite (the anoxic corrosion product of the meteoritic inclusion schreibersite) into mixed ferrocyanide salts and phosphate salts, with counter cations being provided through neutralization and ion-exchange reactions with bedrock and other meteoritic oxides and salts.

Cyanosulfidic chemistry

Chemistry in a post-meteoritic-impact scenario.
A series of post-impact environmental events are shown along with the chemistry (boxed) proposed to occur as a consequence of these events.

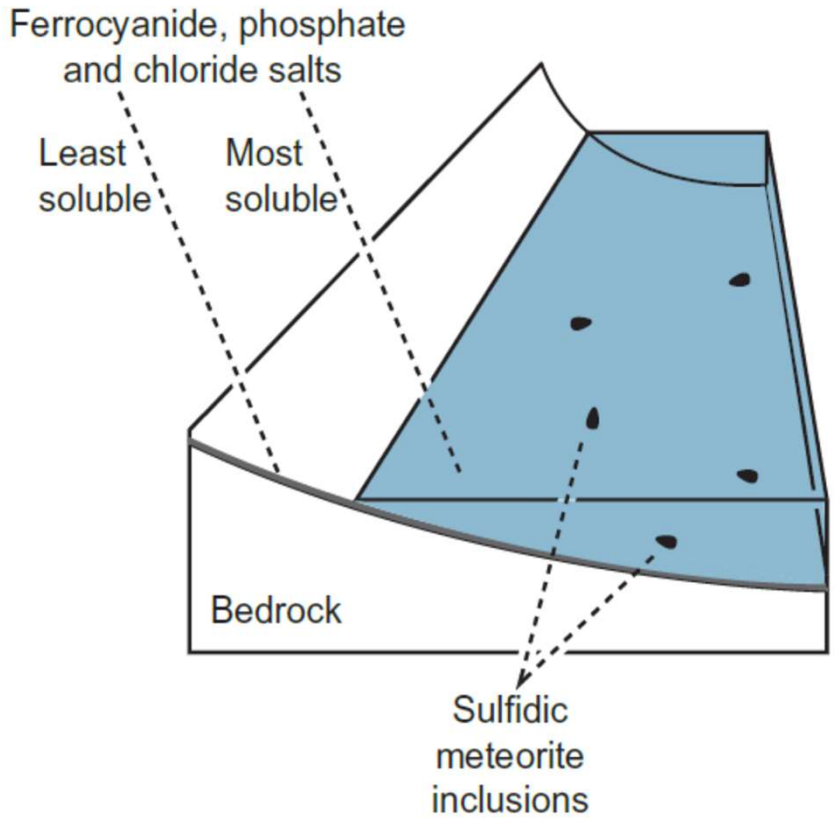

Partial evaporation results in the deposition of the least-soluble salts over a wide area, and further evaporation deposits the most-soluble salts in smaller, lower-lying areas.

Cyanosulfidic chemistry

After complete evaporation, impact or geothermal heating results in thermal metamorphosis of the evaporite layer, and the generation of feedstock precursor salts (in bold).

$$(Na,K)_4[Fe(CN)_6] \xrightarrow{700\ ^\circ C} 4(\mathbf{Na/K})\mathbf{CN} + Fe(CN)_2$$

$$3Fe(CN)_2 \xrightarrow{700\ ^\circ C} Fe_3C + 5C + 3N_2$$

$$Fe(CN)_2 \xrightarrow{700\ ^\circ C} Fe + 2C + N_2$$

$$Mg_2[Fe(CN)_6] \xrightarrow{315\ ^\circ C} 2Mg(CN)_2 + Fe(CN)_2$$

$$Mg(CN)_2 \xrightarrow{395\ ^\circ C} MgCN_2 + C$$

$$3MgCN_2 \xrightarrow{420\ ^\circ C} \mathbf{Mg_3N_2} + 3C + 2N_2$$

$$Ca_2[Fe(CN)_6] \xrightarrow{660\ ^\circ C} 2Ca(CN)_2 + Fe(CN)_2$$

$$Ca(CN)_2 \xrightarrow{660\ ^\circ C} \mathbf{CaNCN} + C \underset{}{\overset{1{,}000\ ^\circ C}{\rightleftharpoons}} \mathbf{CaC_2} + N_2$$

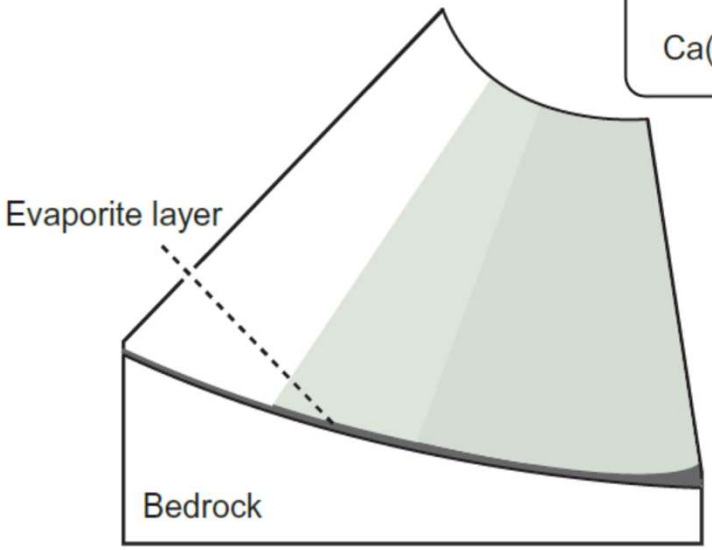

Cyanosulfidic chemistry

Rainfall on higher ground (left) leads to rivulets or streams that flow downhill, sequentially leaching feedstocks from the thermally metamorphosed evaporite layer. Solar irradiation drives photoredox chemistry in the streams. Convergent synthesis can result when streams with different reaction histories merge (right), as illustrated here for the potential synthesis of arabinose aminooxazoline (5) at the confluence of two streams that contained glycolaldehyde (1), and leached different feedstocks before merging.

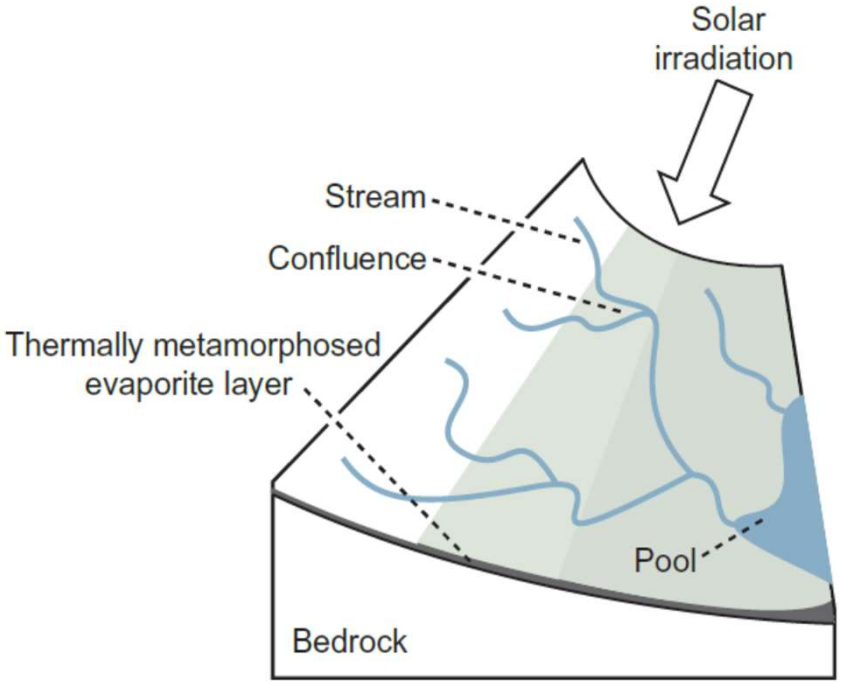

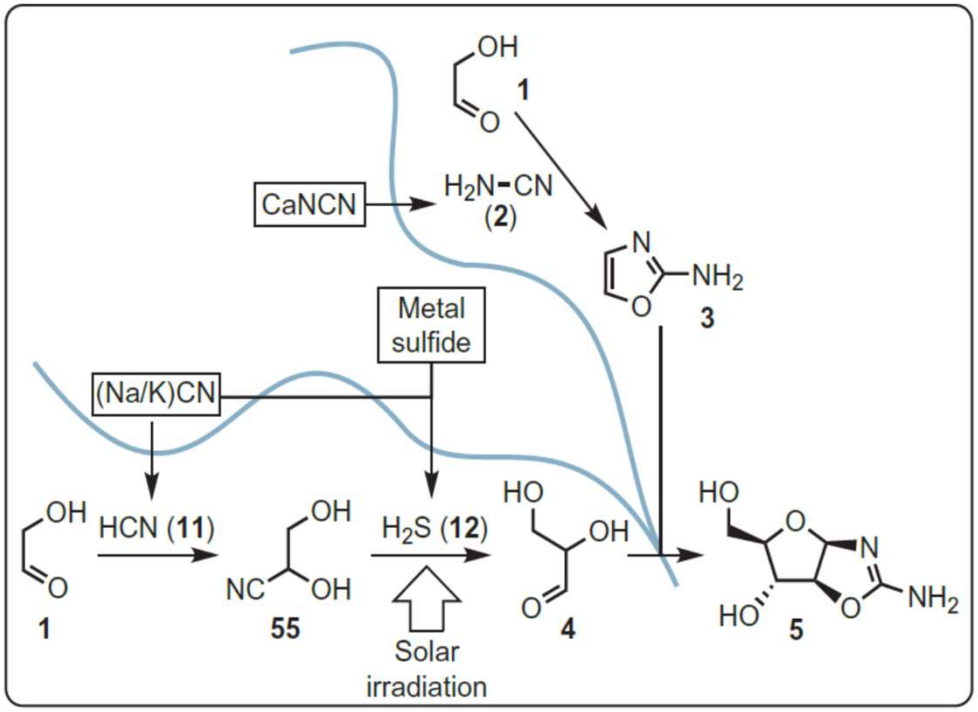

Cyanosulfidic chemistry system

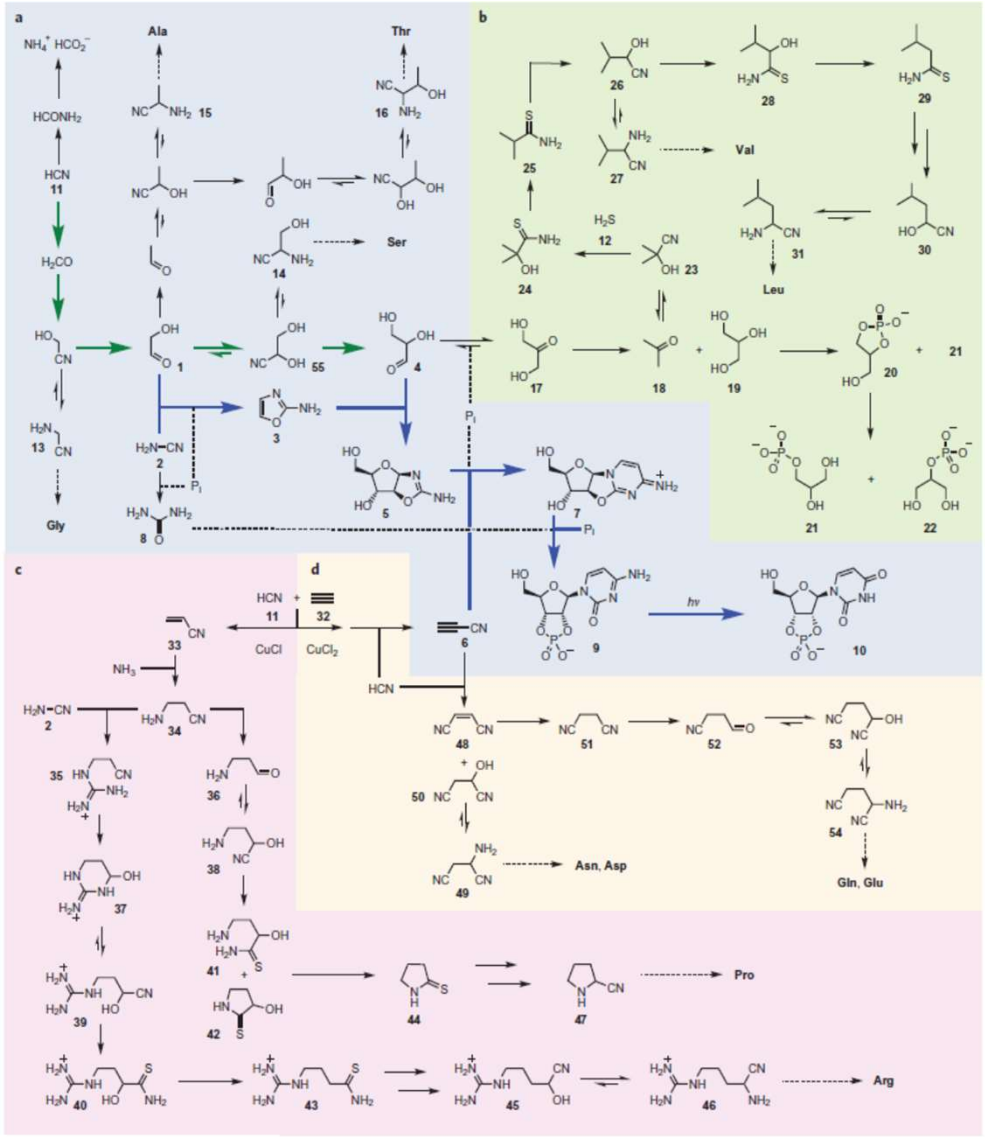

Table 1 | Yields for the part of the reaction network shown in Fig. 1b.

Conversion	Number of steps	Yield (%)	Conversion	Number of steps	Yield (%)
4 → 17	1	59	26 → 28	1	57
17 → 18 + 19	1	29 34	28 → 29	1	75
18 → 24	2	62	26 → 29	2	43
24 → 25	1	41	29 → 30	2	66
25 → 26	2	78	30 → 31	1	42
26 → 27	1	42	19 → 21 + 22	2	31 40

Table 2 | Yields for the parts of the reaction network shown in Fig. 1c,d.

Conversion	Number of steps	Yield (%)	Conversion	Number of steps	Yield (%)
33 → 34	1	83	38 → 41 + 42	1	30 60
34 → 35	1	55	38 → 44	2	70
34 → 37	2	77	44 → 47	2	32
34 → 36	1	45	45 → 46	1	90
37 → 39	1	77	6 → 48 + 49 + 50	1	50 25 16
37 → 40	2	~100	48 → 51	1	90
37 → 43	3	~70	51 → 52	1	89
37 → 45	5	~50	52 → 53	1	~100
36 → 38	1	~100	52 → 54	2	~70

Cyanosulfidic chemistry system

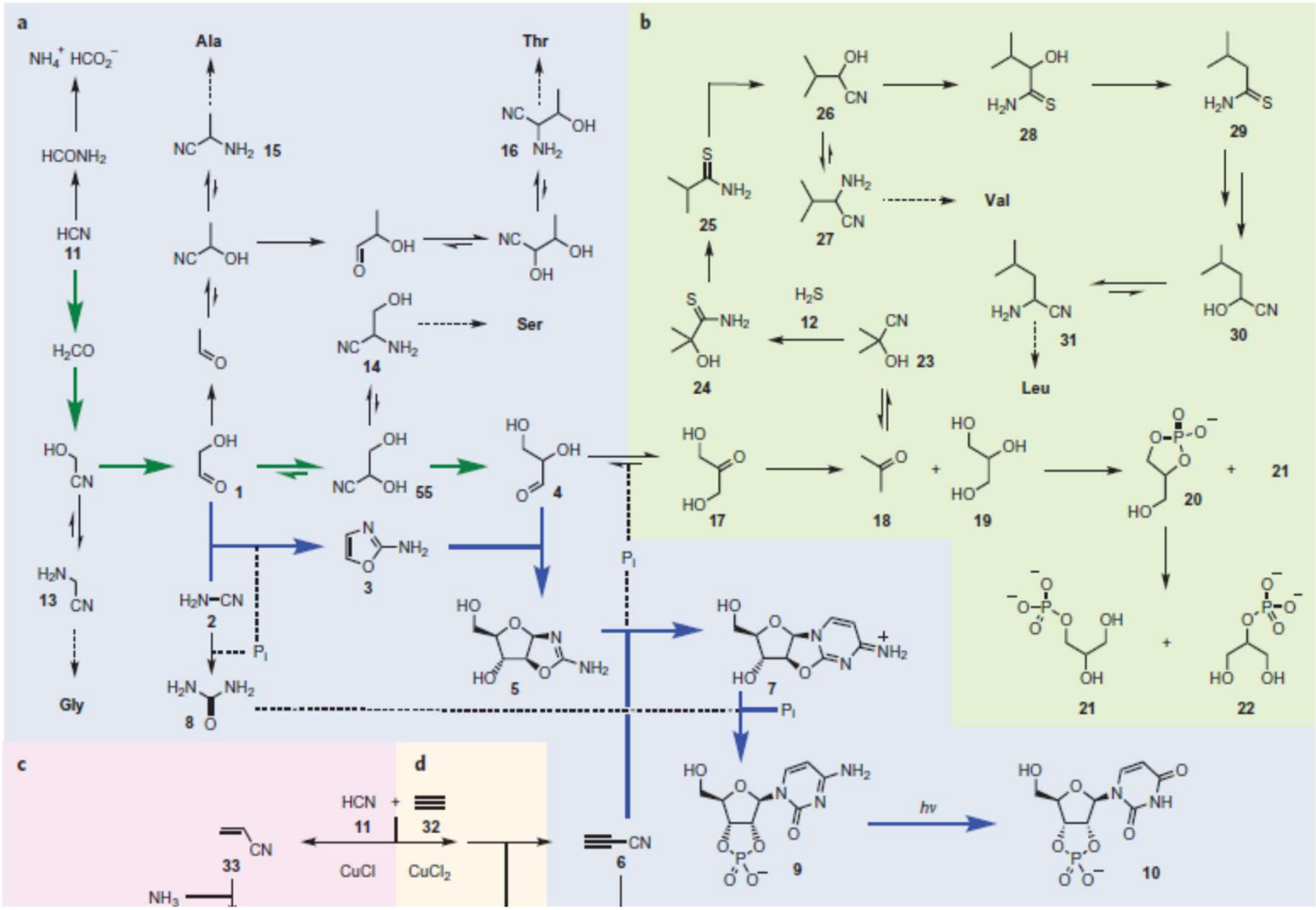

Cyanosulfidic chemistry system

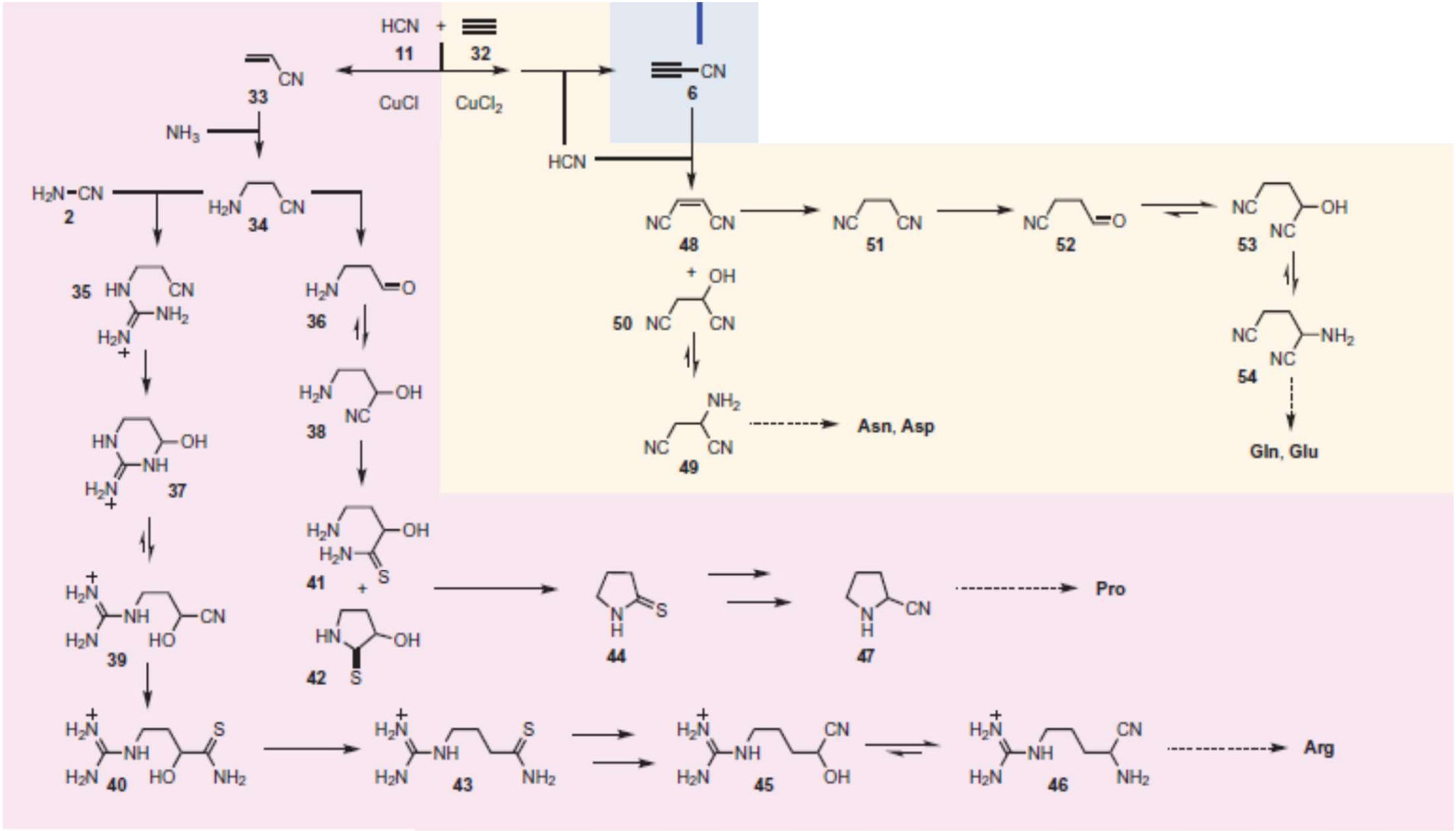

Remaining challenges of prebiotic nucleotide synthesis

Homochirality of currently known biomolecules

Prebiotic synthesis of purine nucleotides and deoxyribonucleotides

Prebiotic polymerization

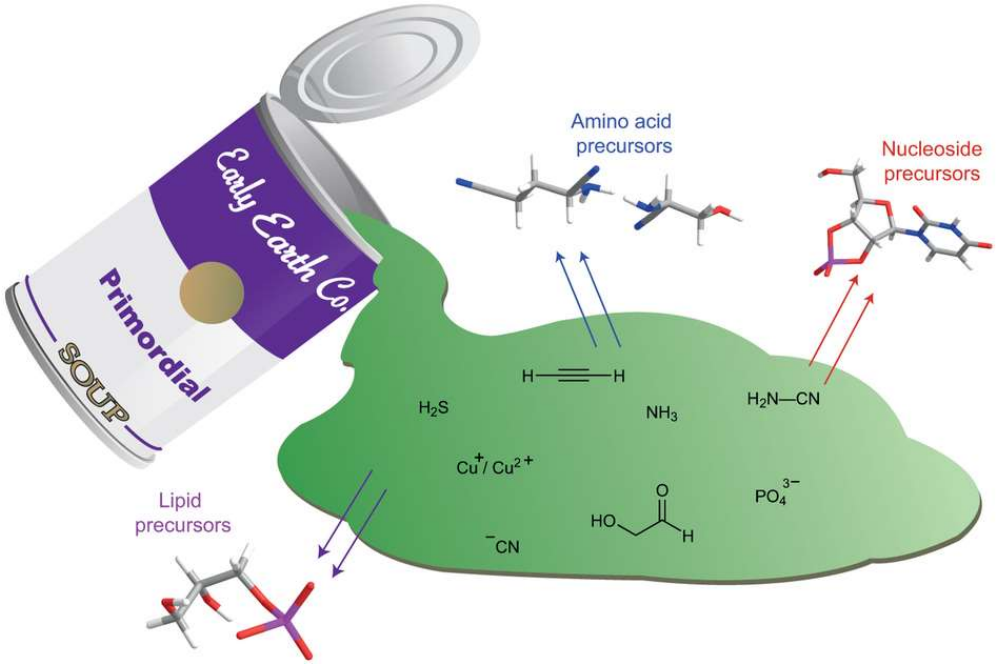

Enantiomeric excess in the cyanosulfidic chemistry

Polymerization of *D*-nucleotides is suppressed in presence of *L*-nucleotides – the problem of „enantiomeric cross-inhibition"

Incorporation of *L*-enantiomers into growing chains of *D*-oligonucleotides → families of diastereomers for each sequence → problematic development of phenotypic RNA properties

Without access to highly enantioenriched sugars, the nucleotides formed during the ‚cyanosulfidic chemistry' synthesis would not lead to informational polymers capable of establishing a genetic code

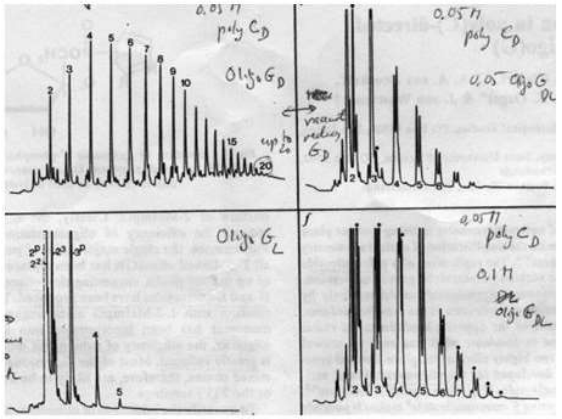

template-directed oligomerization
poly (C_D) → oligo (G_D)

cytosine guanine

→ Mononucleotides with wrong chirality terminate chain growth

ok

poisoned

(using HPLC)

→ *enantiomeric cross-inhibition*

G. F. Joyce, G. M. Visser, C. A. A. Van Boeckel, J. H. Van Boom, L. E. Orgel, J. Van Westrenen, *Nature* **1984**, *310*, 602-604

Chiral amplification and the origins of homochirality

Enantioenriched aminoacids present in meteorites (up to 18 % ee *L*-isomers). Further enantioenrichment is possible by manipulation of aminoacid phase behavior:

Table 1. Enantiomeric concentration amplification of phenylalanine after two crystallizations from water

Component	Initial ee, %	Final ee, %
D	10	90.0 ± 3.7
	5	91.7 ± 1.5
	1	87.2 ± 2.0
L	10	88.3 ± 1.1
	5	88.6 ± 0.9
	1	90.9 ± 0.3

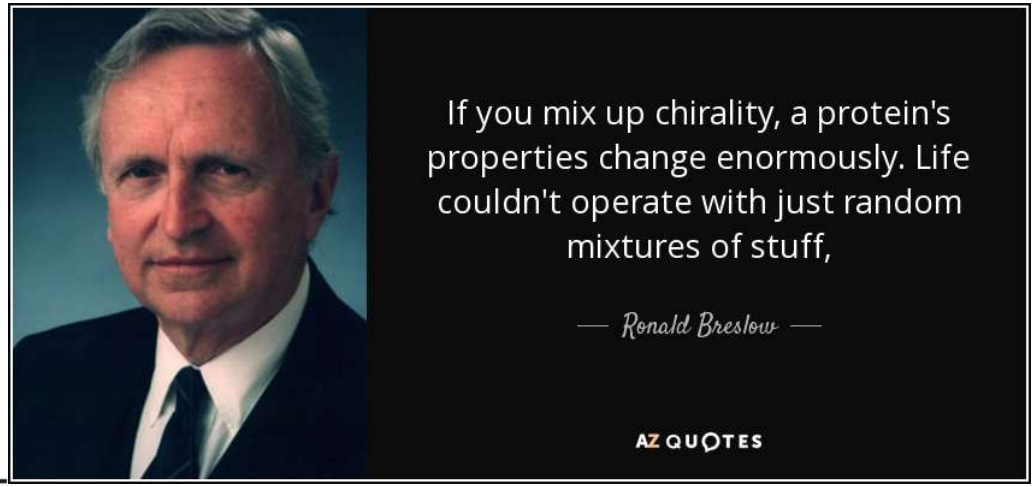

Solutions with as little as 1% enantiomeric excess (ee) of D- or L-phenylalanine are amplified to 90% ee (a 95/5 ratio) by two successive evaporations to precipitate the racemate. Such a process on the prebiotic earth could lead to a mechanism by which meteoritic chiral α-alkyl amino acids could form solutions with high ee values that were needed for the beginning of biology.

Prof. Ronald Breslow
Columbia University, USA

Breslow, R., Levine, M. Proc. Natl. Acad. Sci. USA **2006,** *103(35),* 12979-12980

Eutectic solutions over enantioenriched aminoacids

Mixtures of enantiomers can crystallize as conglomerates (a single crystal contains only molecules of one handedness) or racemates (a single crystal is racemic).

Enantioenriched mixtures give mixtures of crystals which would have the same ee value upon re-solubilization

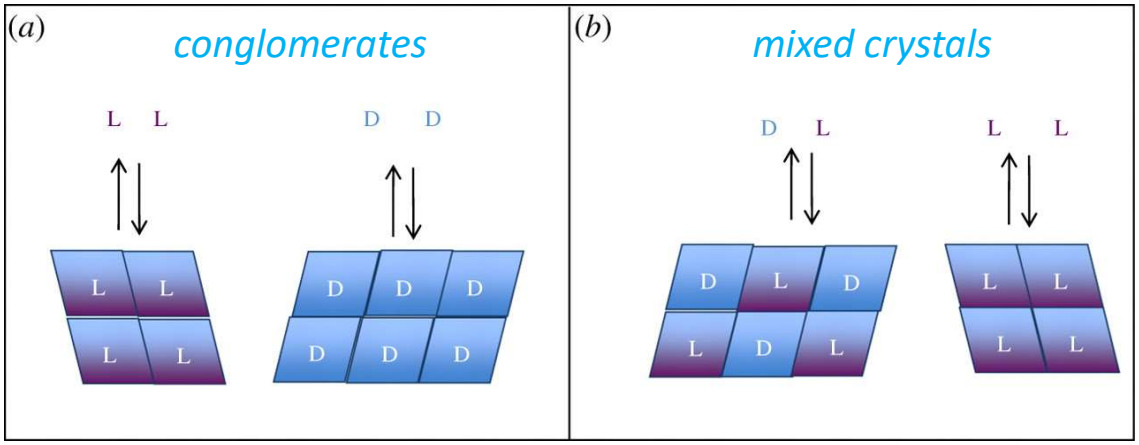

Highly enantioenriched solutions may be obtained from a small initial enantiomeric imbalance for many aminoacids, including proline, via physical amplification processes that sequester the minor enantiomer as racemic solid.

Manipulation of eutectic ee value by formation of a solvate that reduces the solubility of the racemic compound

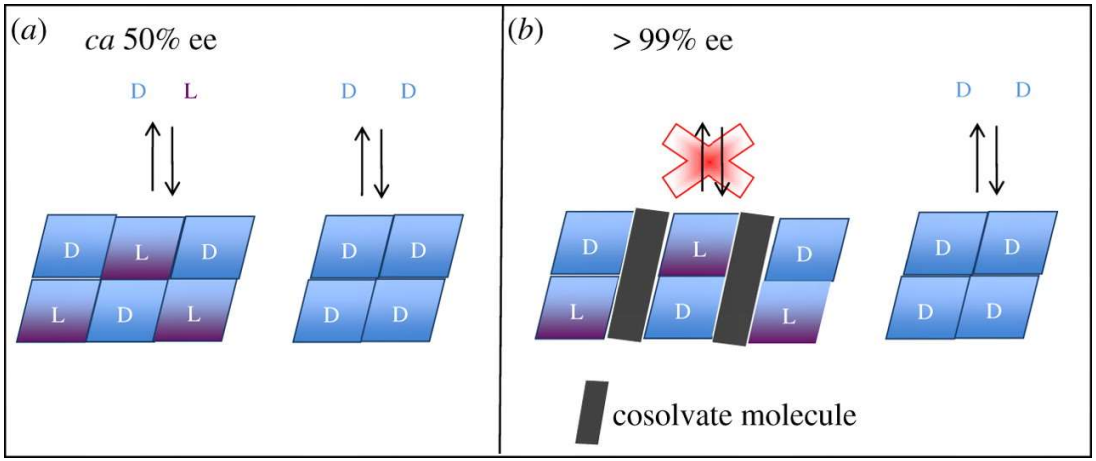

D. Blackmond *Phil. Trans. R. Soc. B* **2011,** *366,* 2878-2884

Eutectic solutions over enantioenriched aminoacids

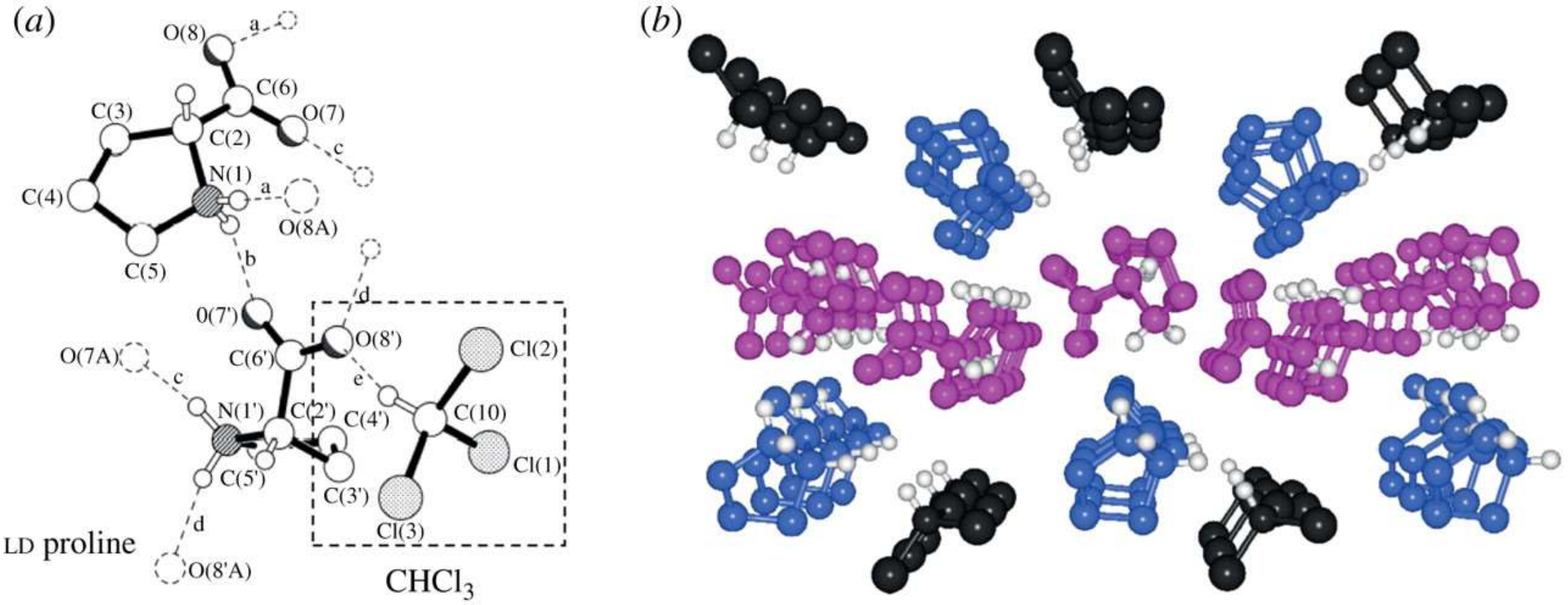

D. Blackmond *Phil. Trans. R. Soc. B* **2011,** *366,* 2878-2884

Eutectic solutions over enantioenriched aminoacids

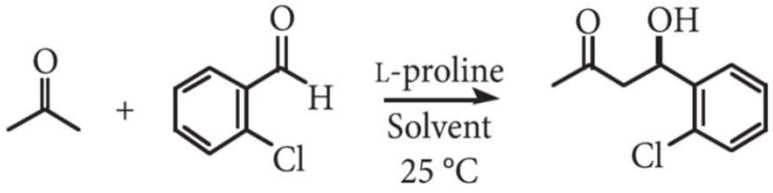

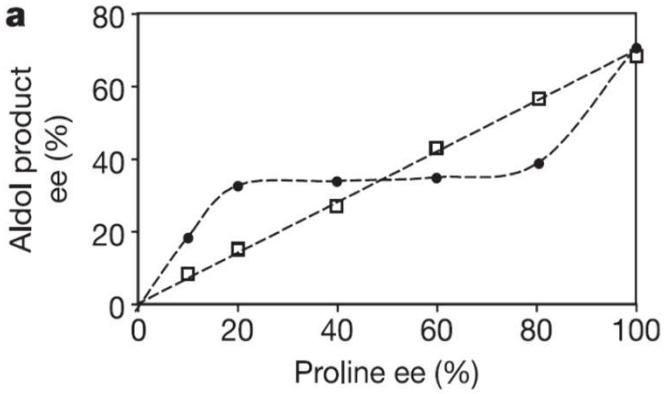

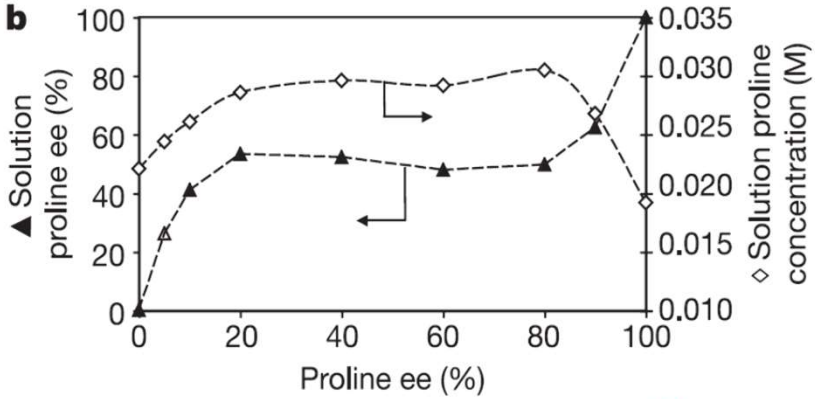

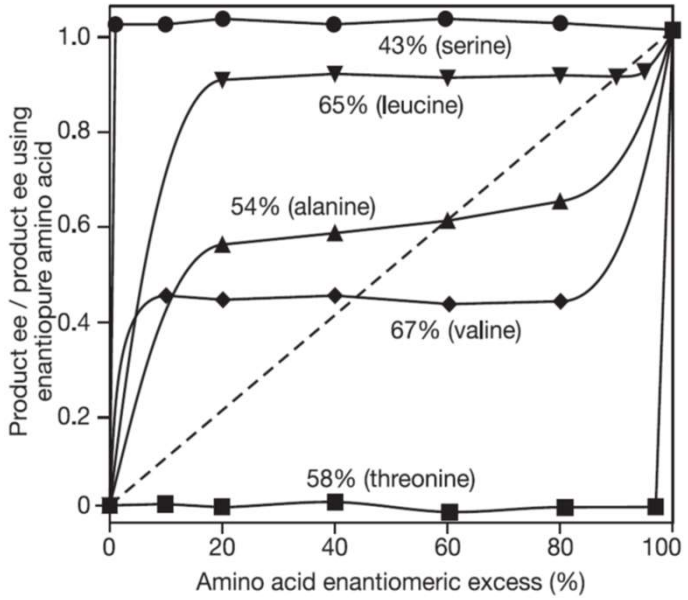

Table 1 | Solution enantiomeric excess at the eutectic point in water at 25 °C for selected amino acids

Amino acid	ee of solution at eutectic (%)	Amino acid	ee of solution at eutectic (%)
Threonine	0	Methionine	85
Valine	46	Leucine	87
Alanine	60	Histidine	93
Phenylalanine	83	Serine	>99

Klussmann, M., et al. Nature **2006,** *441,* 621-623

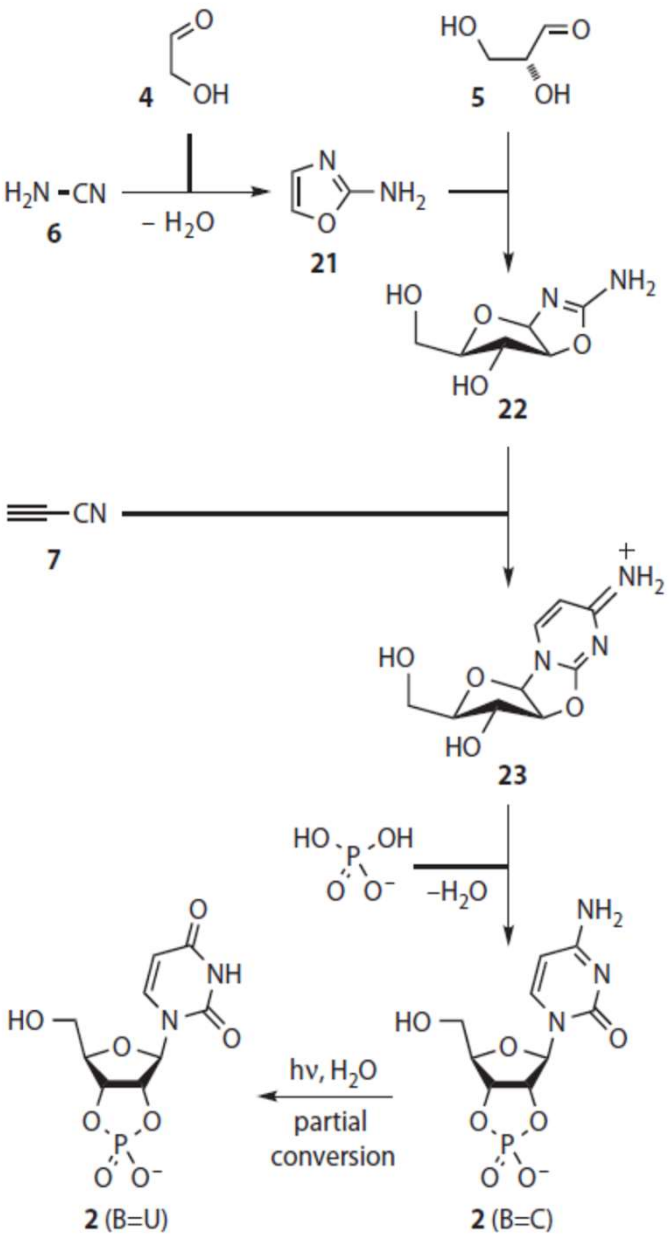

Cyanosulfidic chemistry

The recently uncovered route to activated pyrimidine nucleotides **2**.

The nucleobase ribosylation problem is circumvented by the assembly proceeding through 2-aminooxazole **21**, which can be thought of as the chimera of half a pentose sugar and half a nucleobase. The second half of the pentose - glyceraldehyde **5** -and the second half of the nucleobase—cyanoacetylene **7**—are then added sequentially to give the anhydronucleoside **23**.

Phosphorylation and rearrangement of **23** then furnishes **2** (B=C), and UV irradiation effects the partial conversion of **2** (B=C) to **2** (B=U).

M. W. Powner, B. Gerland, J. D. Sutherland, *Nature* **2009**, *459*, 239–242

Cytosine-2',3'cP – step 2: pentose-amino-oxazolines

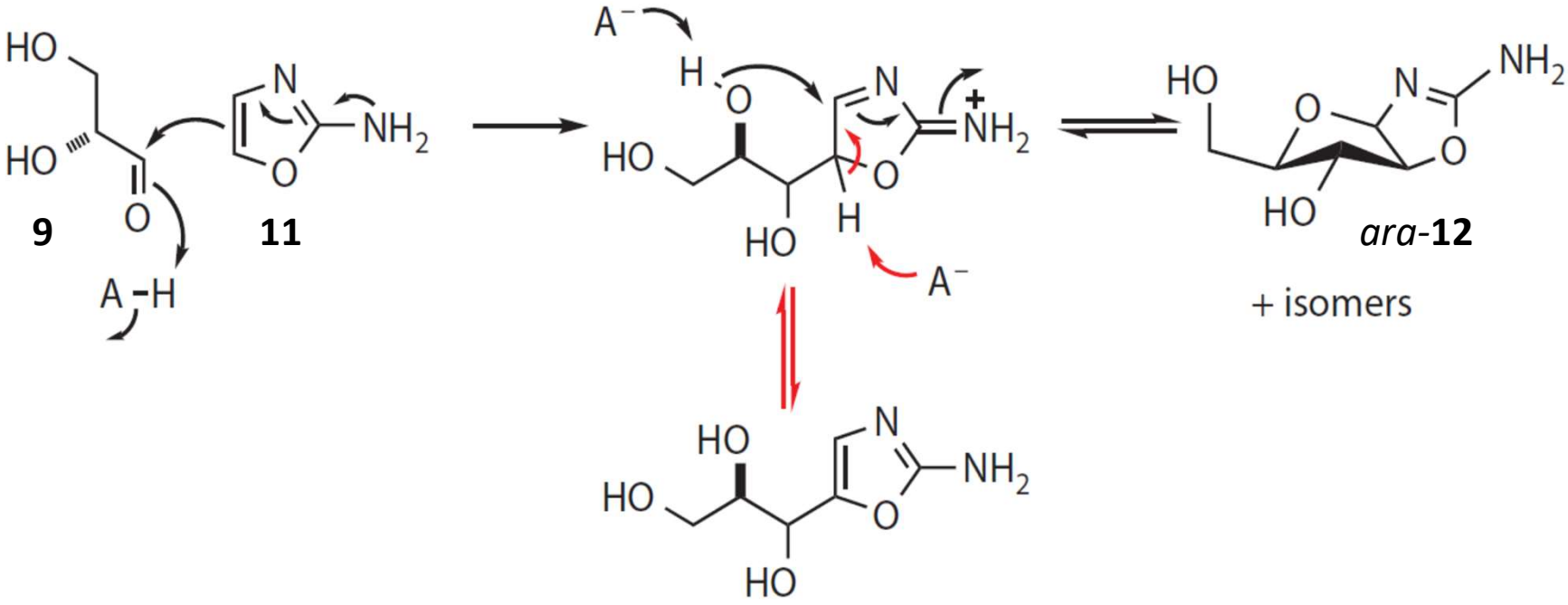

M. W. Powner, B. Gerland, J. D. Sutherland, *Nature* **2009**, *459*, 239–242

Enantiomeric excess in the cyanosulfidic chemistry

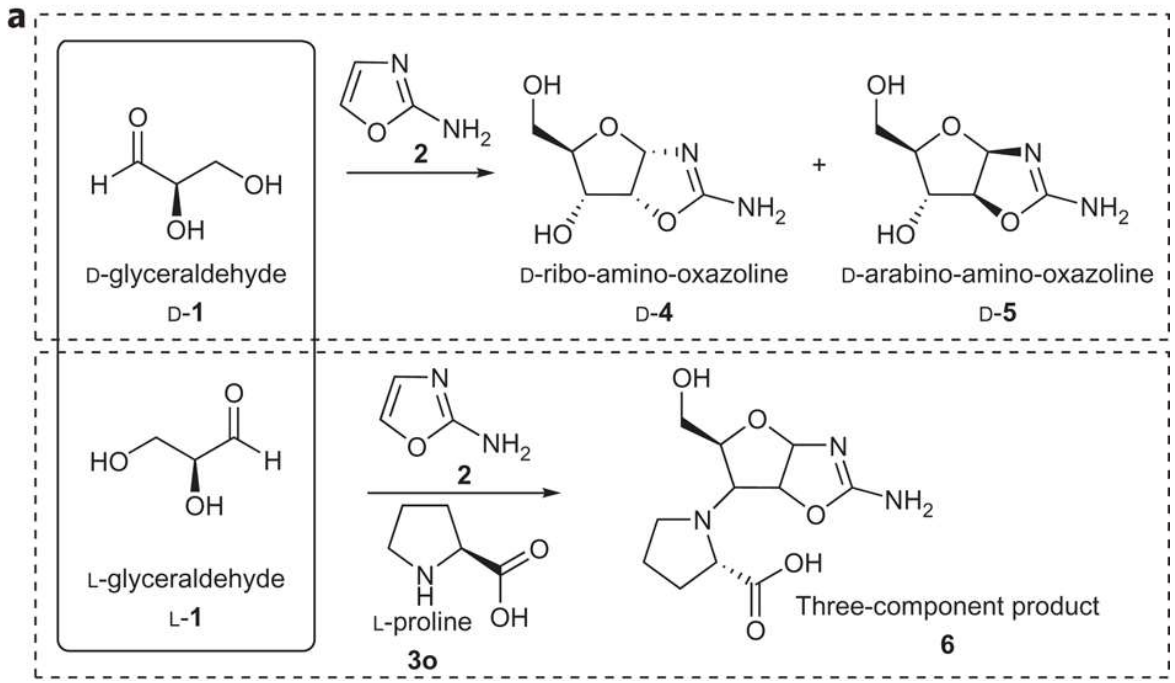

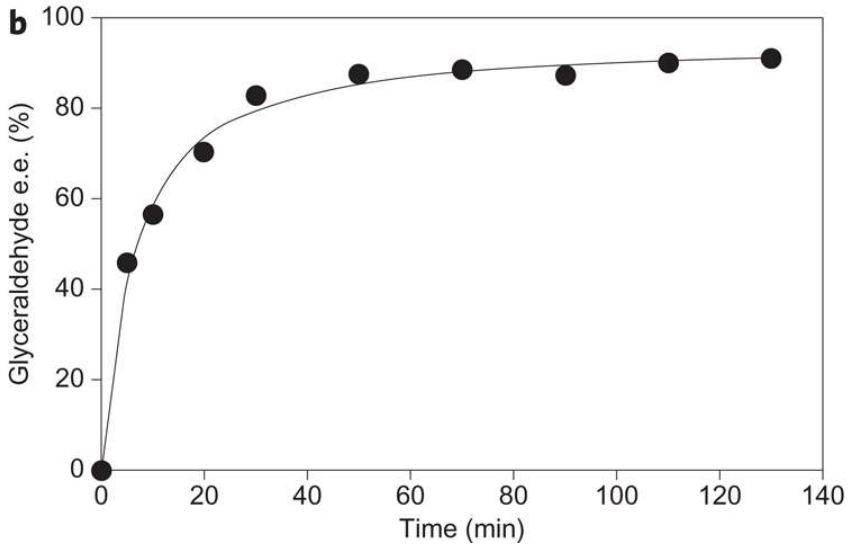

a, In the presence of an enantioenriched L-proline (3o), the diastereoselective formation of a three-component side product (6) effectively sequesters the unnatural L-glyceraldehyde (L-1).

b, The side reaction acts as a kinetic resolution of glyceraldehyde, giving enantiorichment of greater than 90% e.e. D-1, which reacts with 2 to form the enantioenriched amino-oxazoline RNA precursors D-4 and D-5. e.e. values are ±2%.

J. E. Hein, E. Tse, D. G. Blackmond, *Nature Chem.*, **2011**, *3*, 704-706

Enantiomeric excess in the cyanosulfidic chemistry

Table 1 | Formation of enantioenriched amino-oxazolines in the presence of L-amino acids.

Amino acid	Three-component product* 6	Ribose amino-oxazoline D-4 (% e.e.)	Arabinose amino-oxazoline D-5 (% e.e.)
Ala (**3a**)	++	8.9	8.1
Arg (**3b**)	++	4.1	7.3
Asn (**3c**)	+	1.1	0.5
Asp (**3d**)	+	2.1	1.4
Cys (**3e**)	+++	n.a.	1.4
Gln (**3f**)	+	1.2	1.1
Glu (**3g**)	+	0.8	0.1
Gly (**3h**)	++	-	-
His (**3i**)	++	7.5 (L)	8.1 (L)
Ile (**3j**)	+	2.1	0.5 (L)
Leu (**3k**)	+	1.1	2.1
Lys (**3l**)	+++	n.a.	n.a.
Met (**3m**)	+++	n.a.	n.a.
Phe (**3n**)	+++	2.5	5.4
Pro (**3o**)	++	55	58
Ser (**3p**)	+++	3.0	1.9
Thr (**3q**)	++	1.1	2.6
Trp (**3r**)	++	10.2	9.8
Tyr (**3s**)	+	0.5	2.6
Val (**3t**)	++	2.0	1.0 (L)

*Yield of side product **6**: +, low; ++, medium; +++, high. n.a., no products isolated or observed by chiral LC

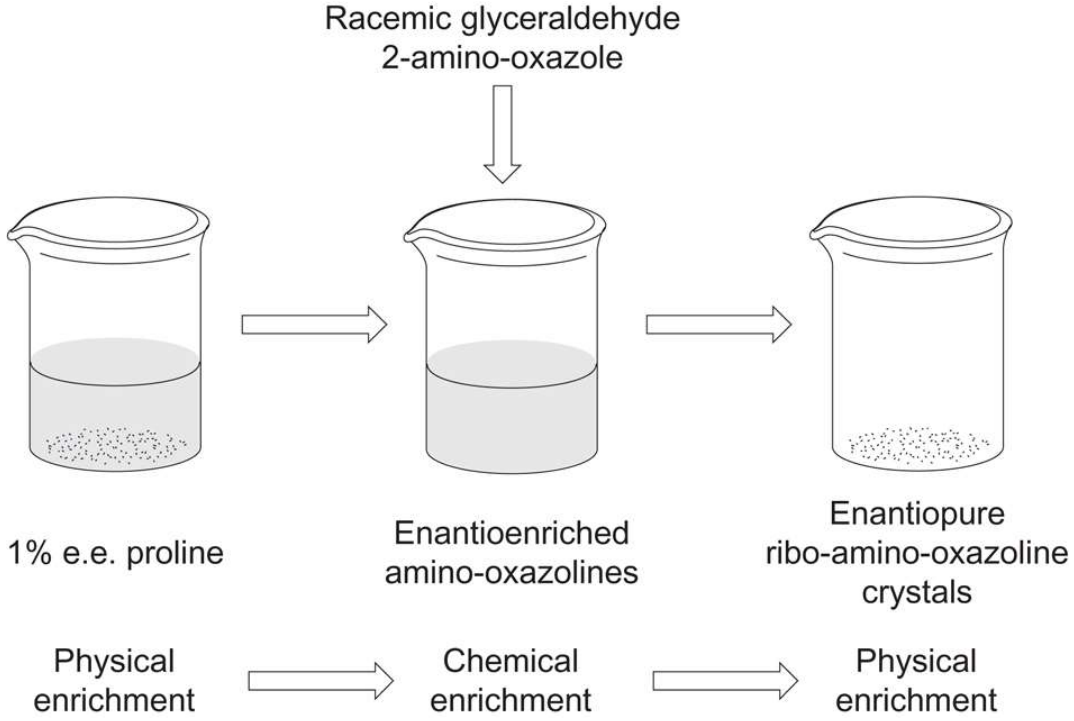

1% e.e. L-proline (3o) is suspended in solvent (either $CHCl_3$ or EtOH). After equilibration, the remaining solid is removed and the solvent is evaporated from the supernatant. Racemic glyceraldehyde DL-**1** and amino-oxazole **2b** are then added and the mixture is dissolved in water. The ensuing reaction produces amino-oxazolines **4** and **5** in 20–80% e.e. Cooling the mixture to 4 °C induces crystallization of enantiopure ribo-amino-oxazoline crystals.

J. E. Hein, E. Tse, D. G. Blackmond, *Nature Chem.*, **2011**, *3*, 704-706

Chiral sugars drive enantioenrichment in prebiotic aminoacid synthesis

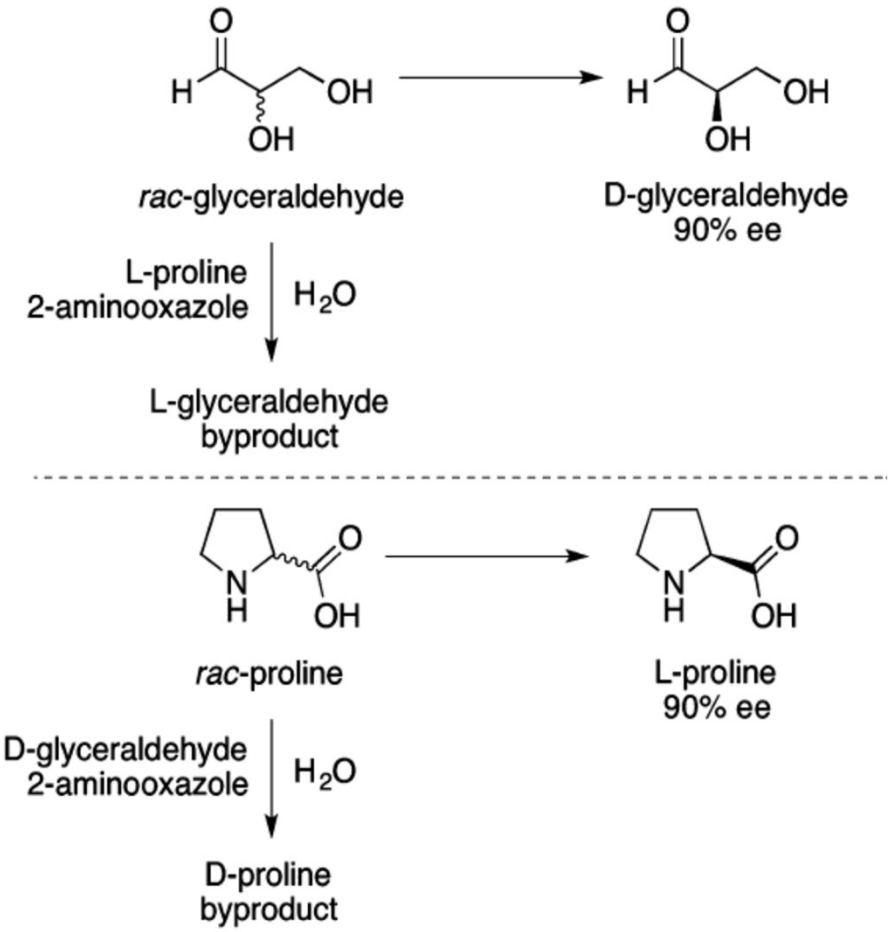

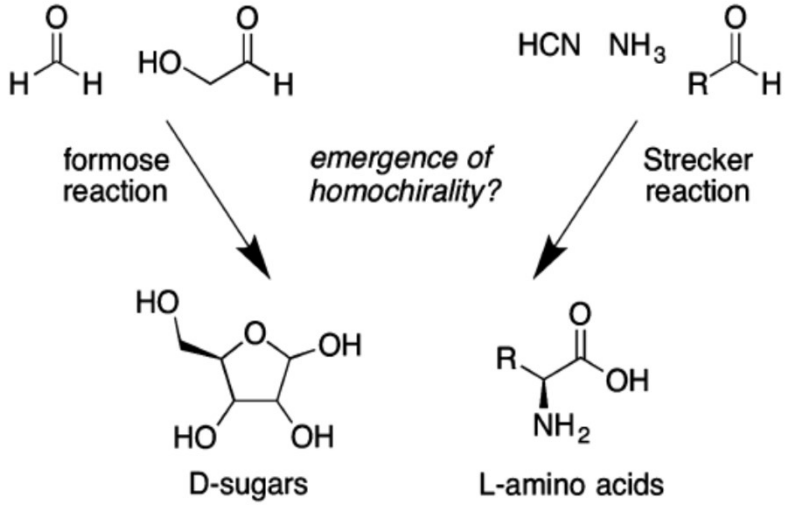

D. G. Blackmond *et al.*, *ACS Cent. Sci.*, **2017**, *3*, 322-328

Chiral sugars drive enantioenrichment in prebiotic aminoacid synthesis

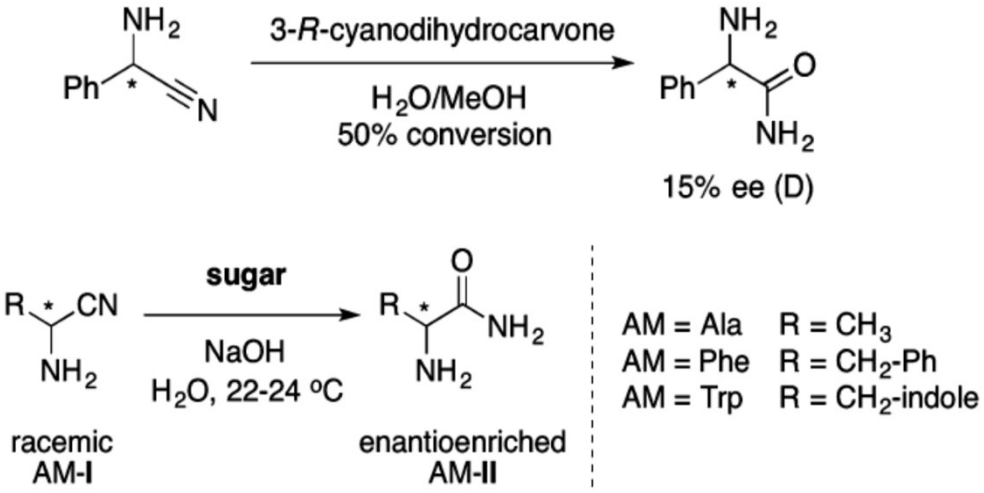

Table 1. Enantioenrichment of Amino Acid Precursors Driven by D-Sugars (Scheme 3)[a]

Sugar	Ala-**II** e.e.(%)	Phe-**II** e.e.(%)	Trp-**II** e.e.(%)
D-ribose 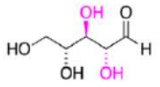	65 (D)	70 (D)	33 (D)
D-lyxose 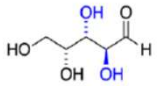	83 (L)	83 (L)	59 (L)
D-xylose 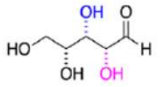	45 (D)	35 (D)	11 (D)
D-arabinose 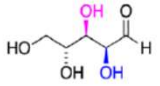	58 (L)	48 (L)	38 (L)
D-deoxyribose 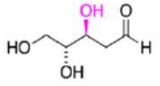	29 (D)	32 (D)	33 (D)
D-ribose + D-lyxose	45 (L)	14 (L)	18 (L)
D-ribose + D-lyxose + D-xylose + D-arabinose	47 (L)	18 (L)	20 (L)

Table 2. Opposite Sense of Enantioenrichment of Phe-II for L-Sugars[a]

Sugar	Phe-**II** e.e. (%)
L-ribose	69 (L)
L-lyxose	81 (D)
L-xylose	31 (L)
L-arabinose	43 (D)

D. G. Blackmond *et al.*, *ACS Cent. Sci.*, **2017**, *3*, 322-328

Chiral sugars drive enantioenrichment in prebiotic aminoacid synthesis

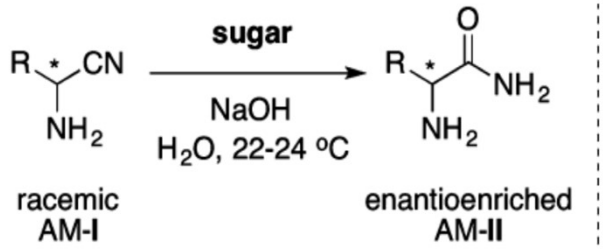

AM = Ala R = CH_3
AM = Phe R = CH_2-Ph
AM = Trp R = CH_2-indole

Table 3. Effect of Sugar Concentration on Phe-II ee (%) for Reaction Mediated by D-Ribose[a]

[D-ribose] (M)	D-ribose (equiv)	Phe-II e.e. (%)
0.025	0.1	9 (D)
0.050	0.2	14 (D)
0.10	0.4	23 (D)
0.25	1	43 (D)
0.5	2	43 (D)
1.0	4	41 (D)
2.0	8	42 (D)

Table 4. Effect of Solution pH on Phe-II ee (%) for Reaction Mediated by D-Ribose[a]

NaOH (M)	Effective pH	Temperature (°C)	Phe-II e.e. (%)
-[b]	7	22-24	35 (D)
-[b]	7	37	46 (D)
0.00010	10	22-24	36 (D)
0.00010	10	37	36 (D)

Scheme 4. Stereochemical Rationalization of Enantioenrichment by Chiral Sugars

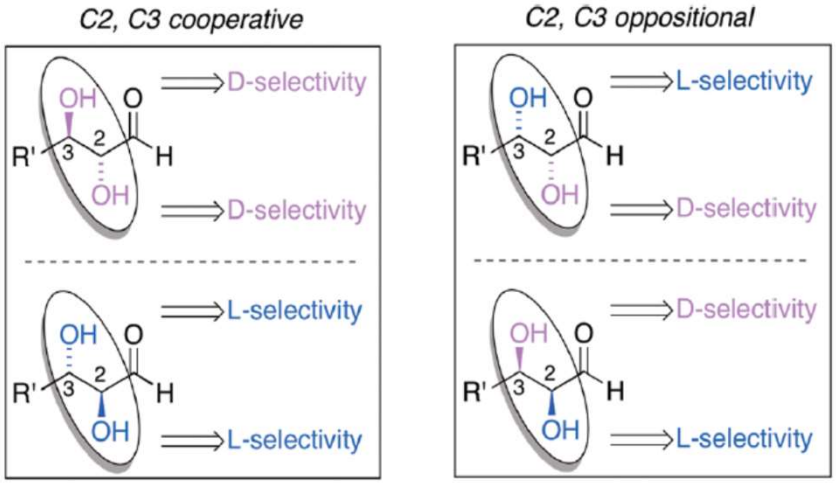

D. G. Blackmond *et al.*, *ACS Cent. Sci.*, **2017**, *3*, 322-328

Chiral sugars drive enantioenrichment in prebiotic aminoacid synthesis

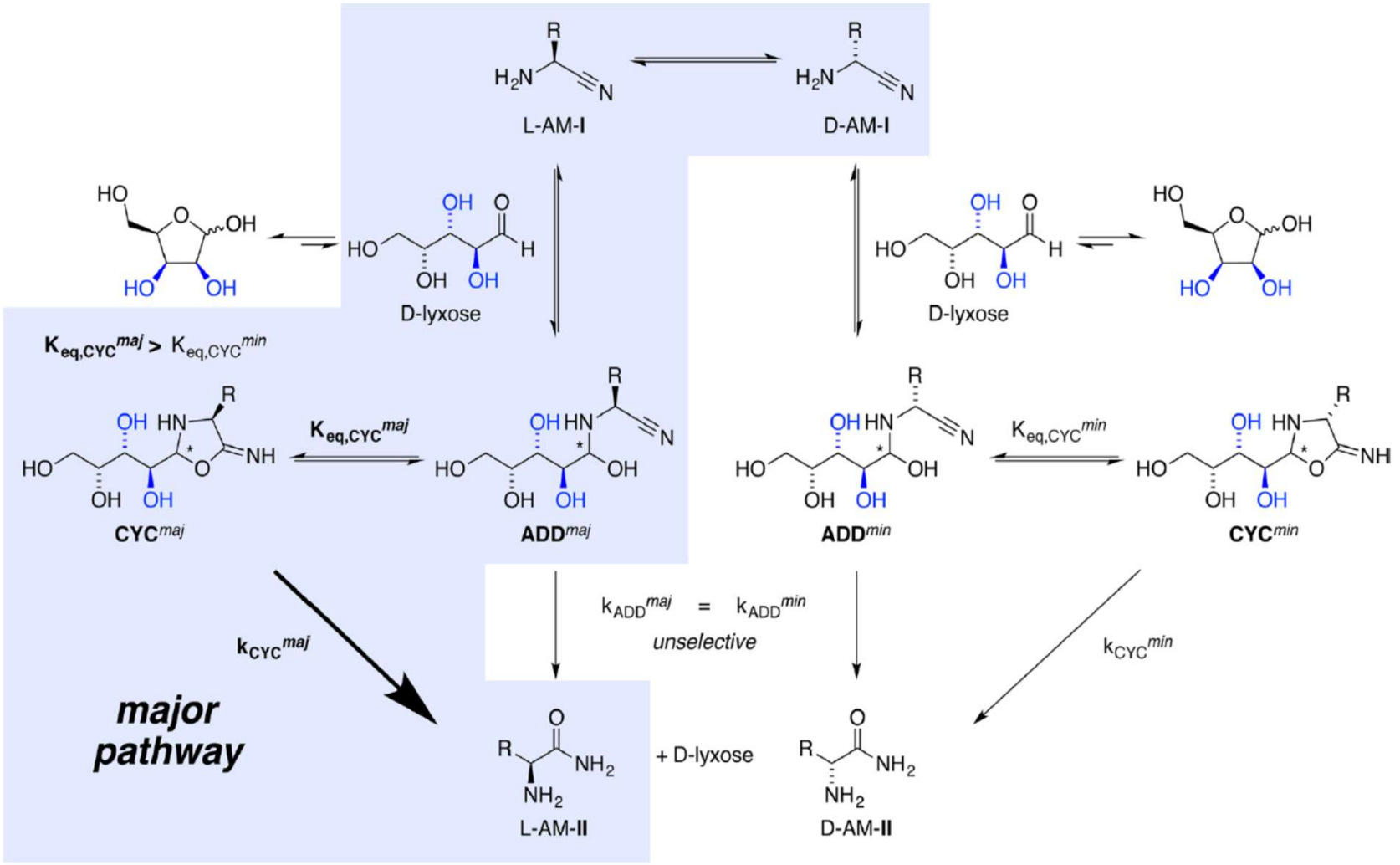

D. G. Blackmond *et al.*, *ACS Cent. Sci.*, **2017**, *3*, 322-328

Nucleoside synthesis – further development

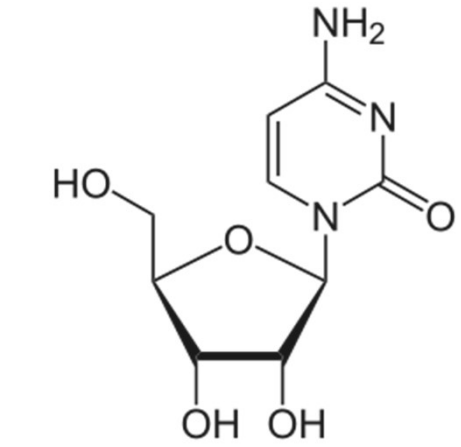

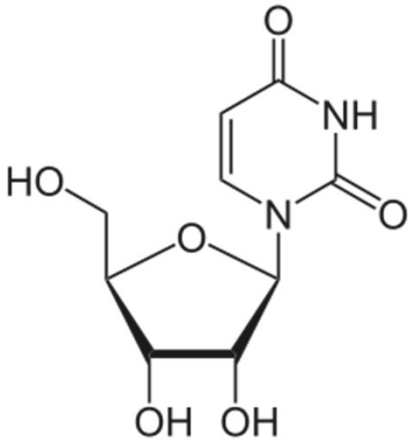

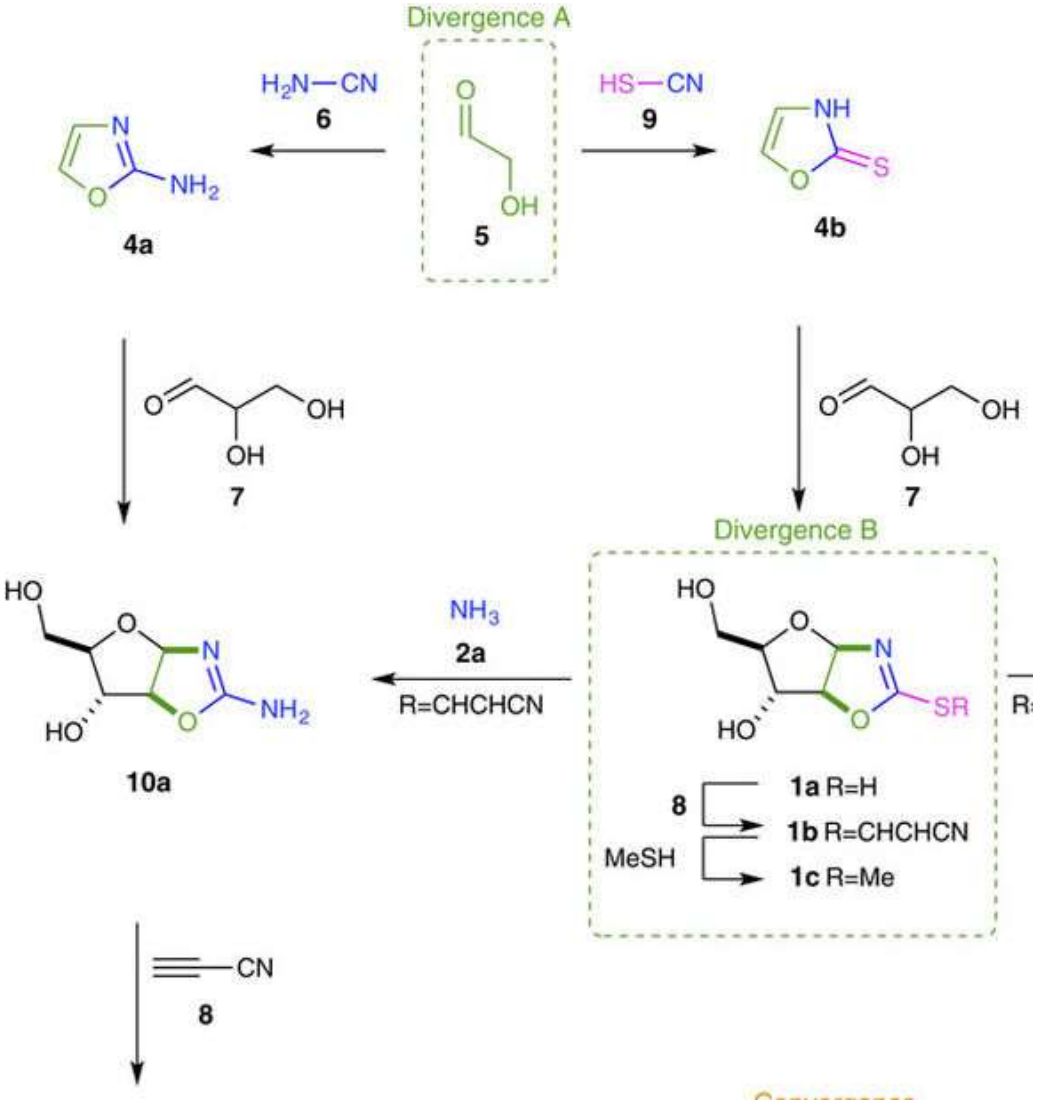

Overcome of the Formation of Prebiotic Clutter.

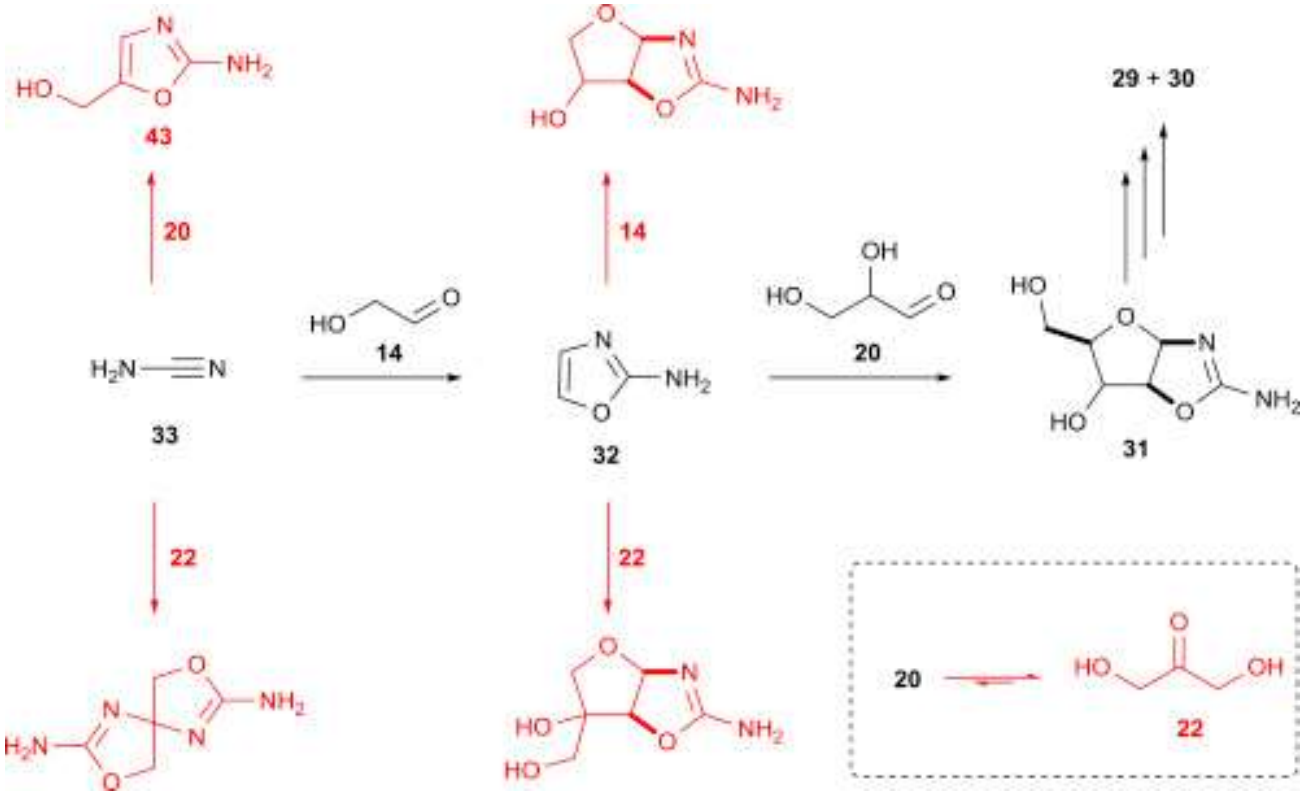

The synthesis of activated pyrimidine ribonucleotides **29** and **30** is dependent on the controlled formation of pentose aminooxazolines **31** (black), but the synthesis of **31** is wholly reliant on the ordered introduction of pure glycolaldehyde **14** (to cyanamide 33) and glyceraldehyde **20** (to 2-aminooxazole **32**) to prevent the formation of numerous deleterious by-products (red). Ribonucleotide synthesis fails without the adherence to this order of synthetic steps.
Glyceraldehyde **20** is highly susceptible to equilibration with dihydroxyacetone **22**, especially in phosphate buffer, which results in diminishing amounts of pentose aminooxazolines **31** being formed (inset).

S. Islam, M. W. Powner *Chem* **2017**, *2*, 470-501

2-Aminothiazole-Controlled Aldehyde Sequestration

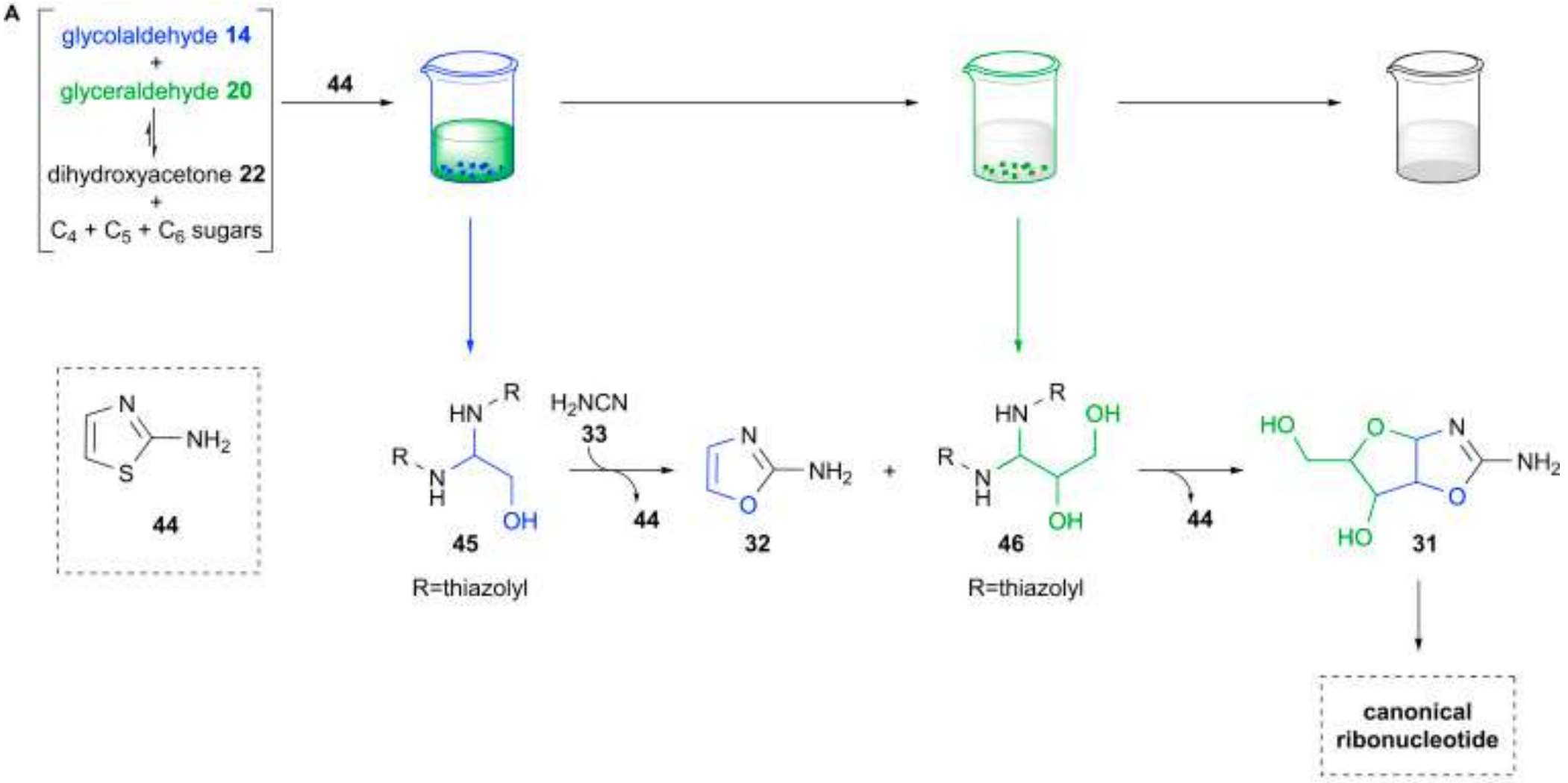

S. Islam, M. W. Powner *Chem* **2017**, *2*, 470-501

2-Aminothiazole-Controlled Aldehyde Sequestration

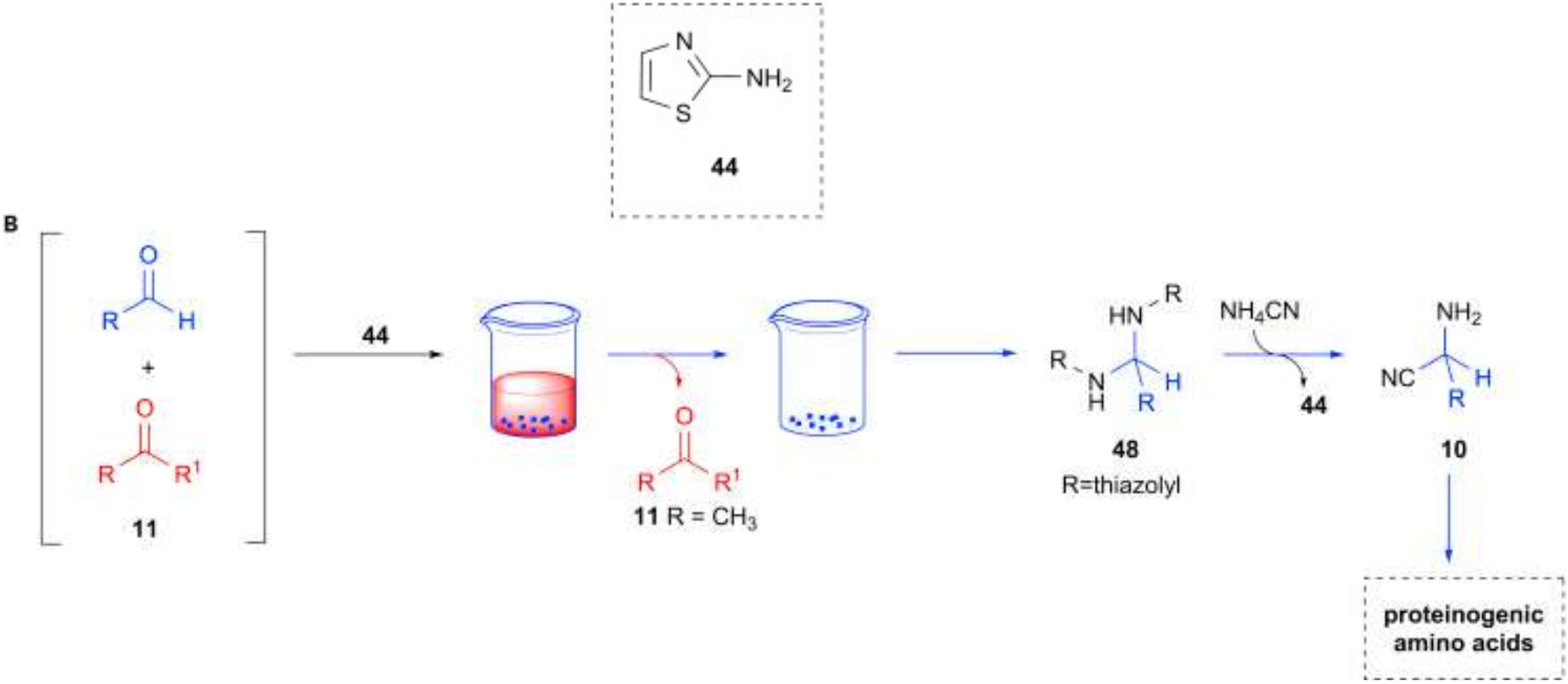

S. Islam, M. W. Powner *Chem* **2017**, *2*, 470-501

Systems Chemical Analysis of Amino Acid and Nucleotide Syntheses

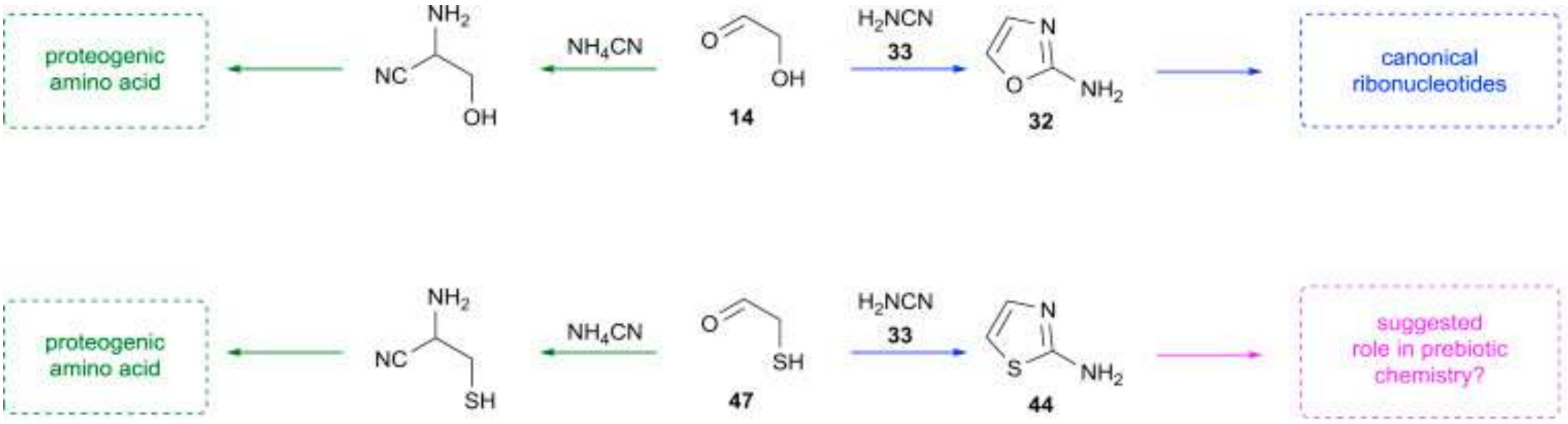

Analysis of the prebiotic amino acid and nucleotide syntheses reveal that glycolaldehyde **14**—a serine and ribonucleotide precursor—lies at a generational node between these two metabolite classes. The same analysis applied to cysteine suggested that b-mercaptoacetaldehyde **47** would be as important as glycolaldehyde **14** and that the reactivity of 2-aminothiazole **44** might have key implications for the concomitant prebiotic synthesis of amino acid and nucleotides

S. Islam, M. W. Powner *Chem* **2017**, *2*, 470-501

Strategies toward Enantio-enriched Glyceraldehyde and Ribonucleotide Precursors

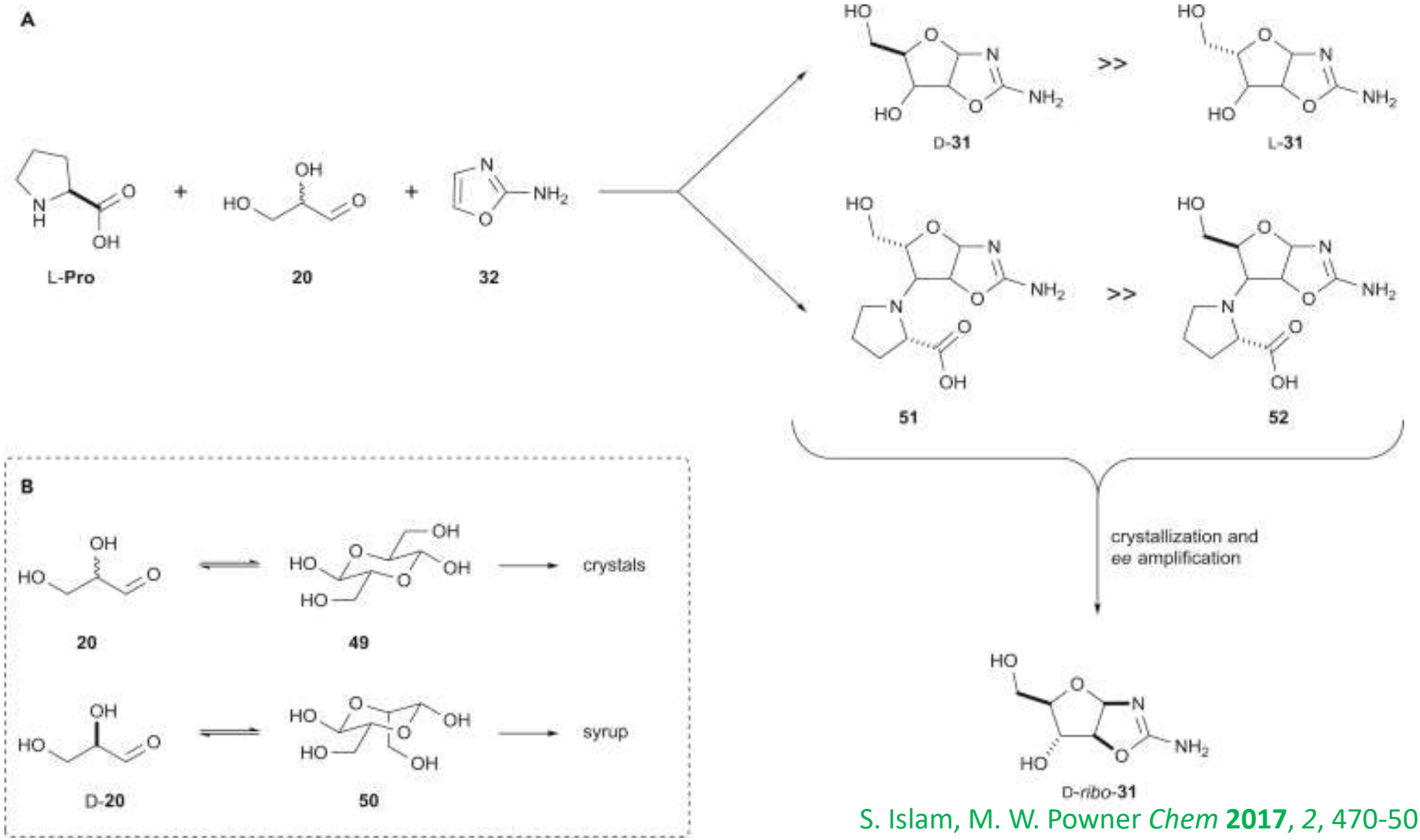

S. Islam, M. W. Powner *Chem* **2017**, *2*, 470-501

Purine nucleoside synthesis via cyanosulfidic chemistry

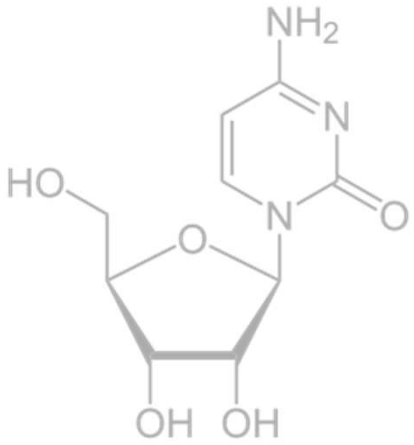

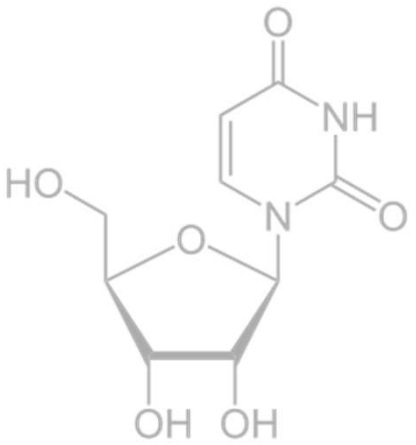

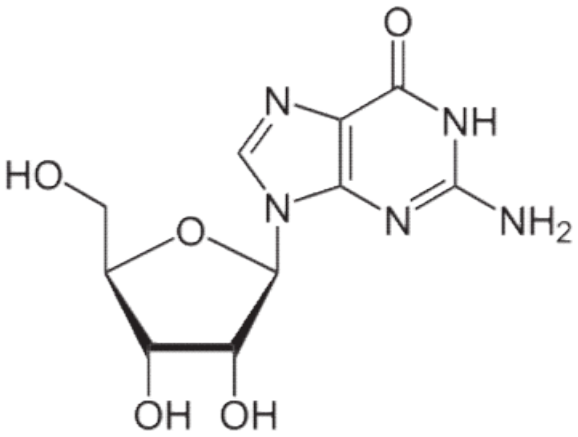

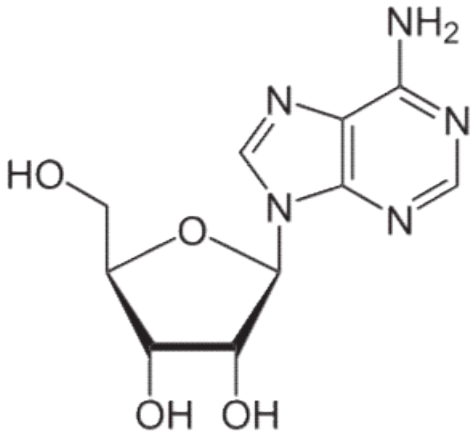

8-Oxo-purine nucleoside synthesis via cyanosulfidic chemistry

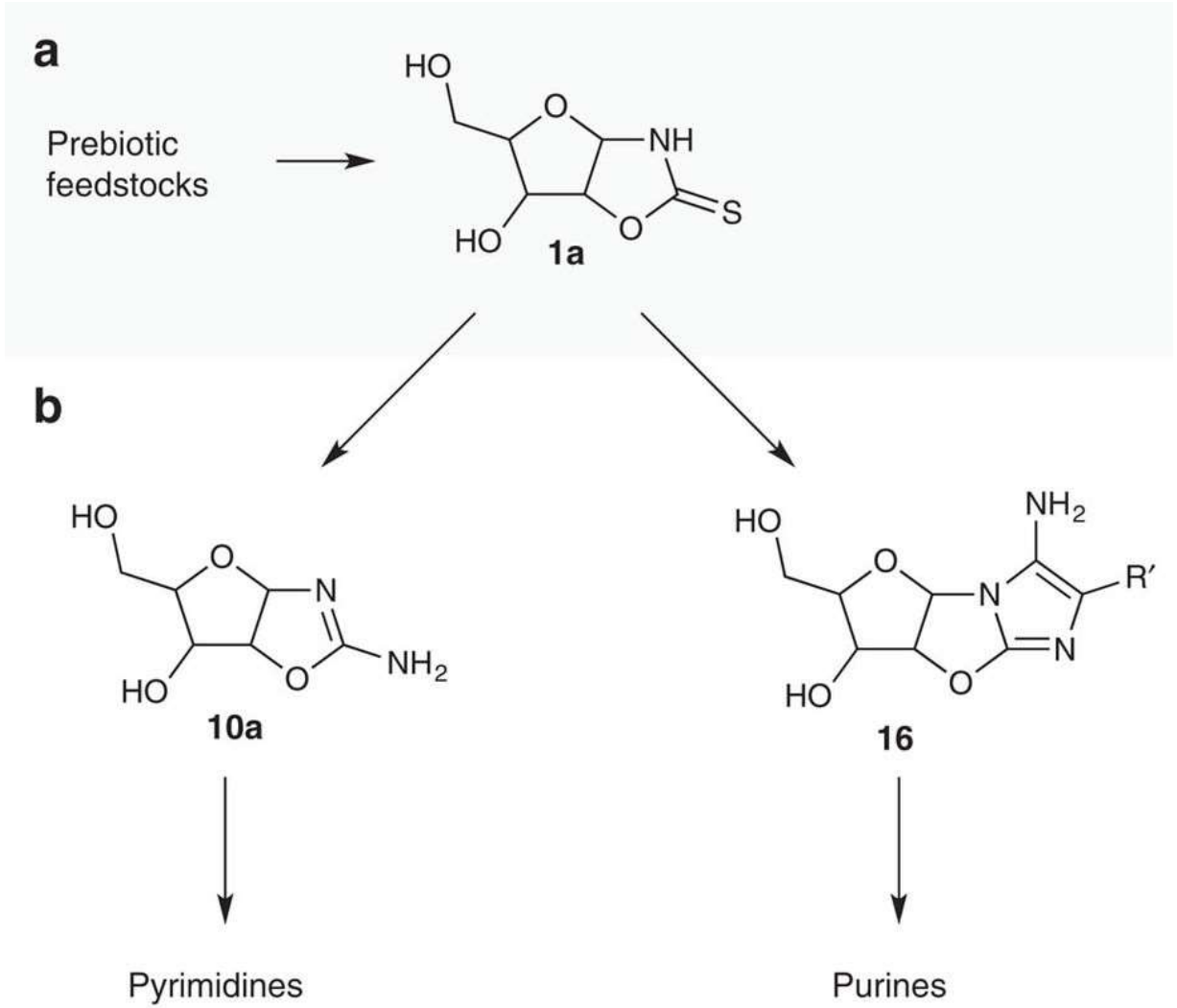

8-Oxo-purine nucleoside synthesis via cyanosulfidic chemistry

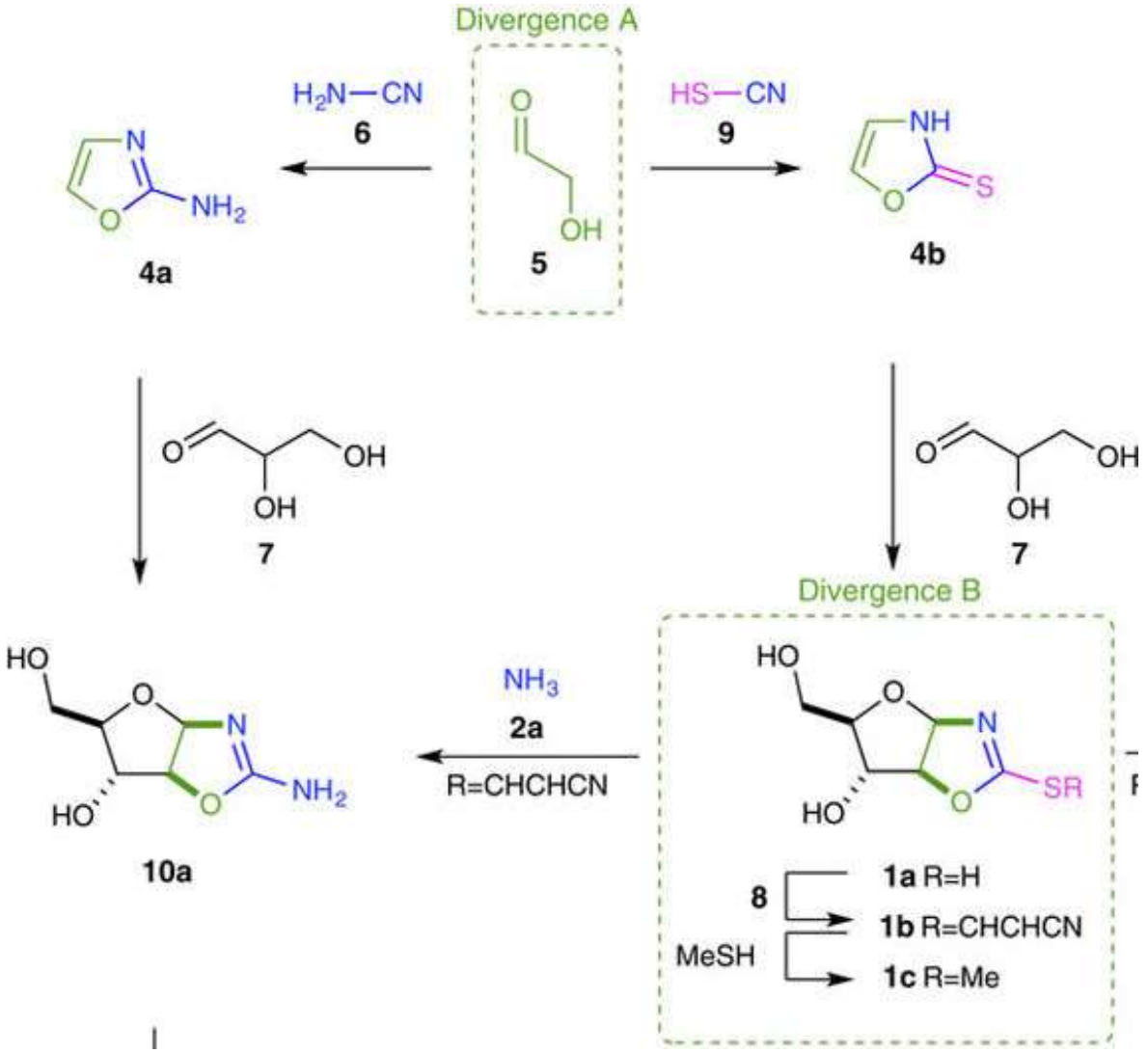

8-Oxo-purine nucleoside synthesis via cyanosulfidic chemistry

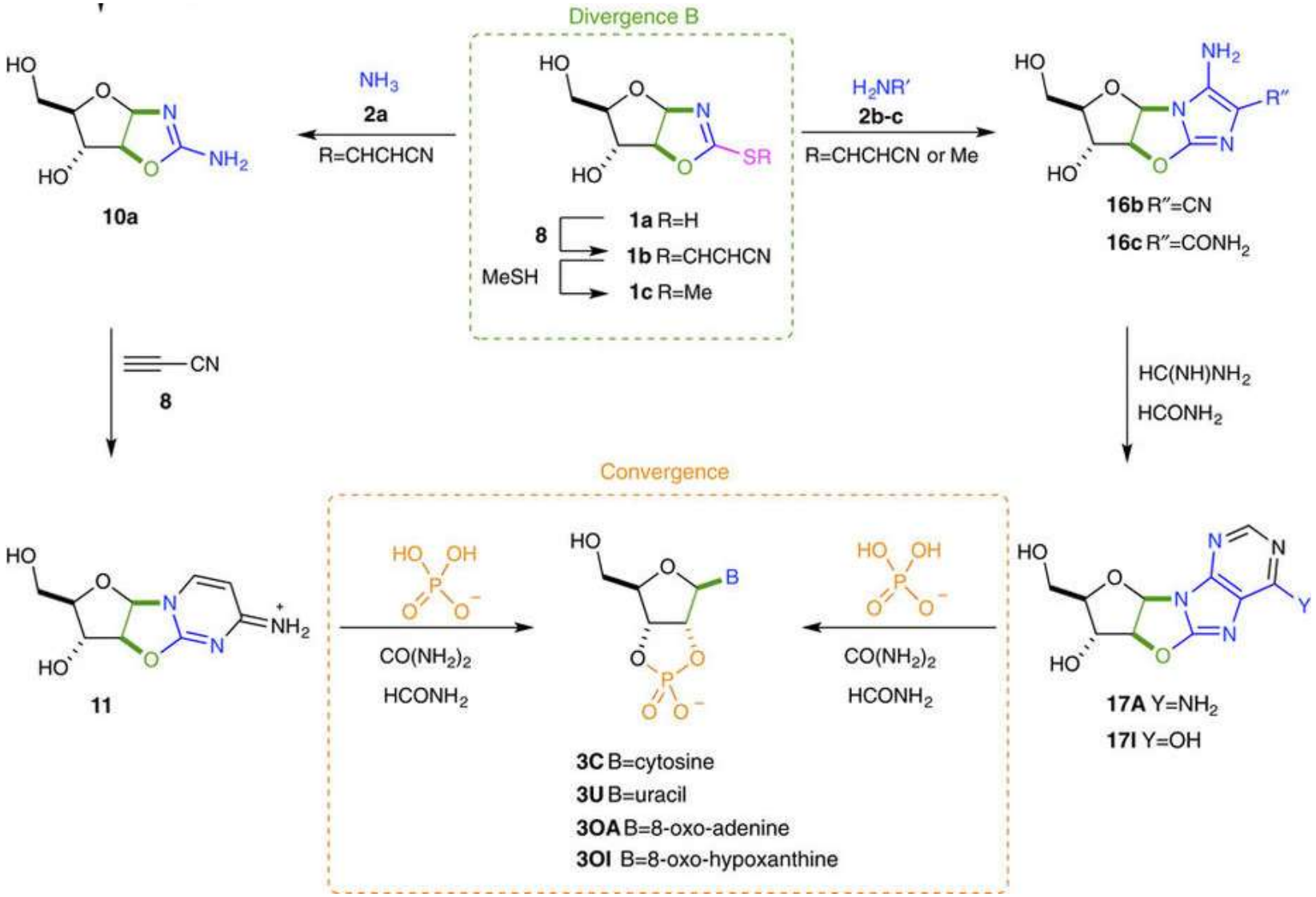

Canonical purine nucleoside synthesis via cyanosulfidic chemistry

Multicomponent Assembly of Hydrogen Cyanide Tetramers

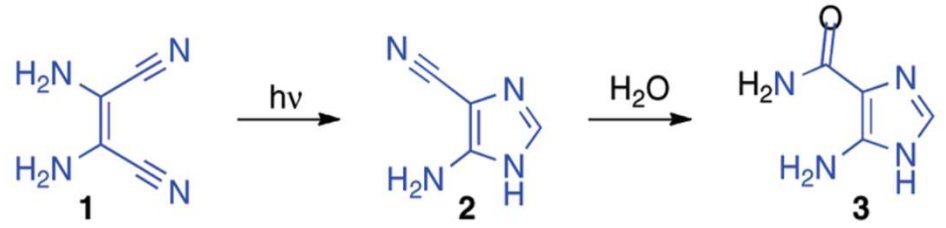

J. Am. Chem. Soc. **2010**, *132*, 16677-16688

Canonical purine nucleoside synthesis via cyanosulfidic chemistry

beta-Ribofuranosyl-pyrimidine nucleotide assembly and potential stepwise, regioselective beta-ribofuranosyl-purine assembly
Pathway via the intermediacy of tetrahydroimidazo[1′,3′]-2′′-aminooxazolo[1′,2′]-pyrimidinesa

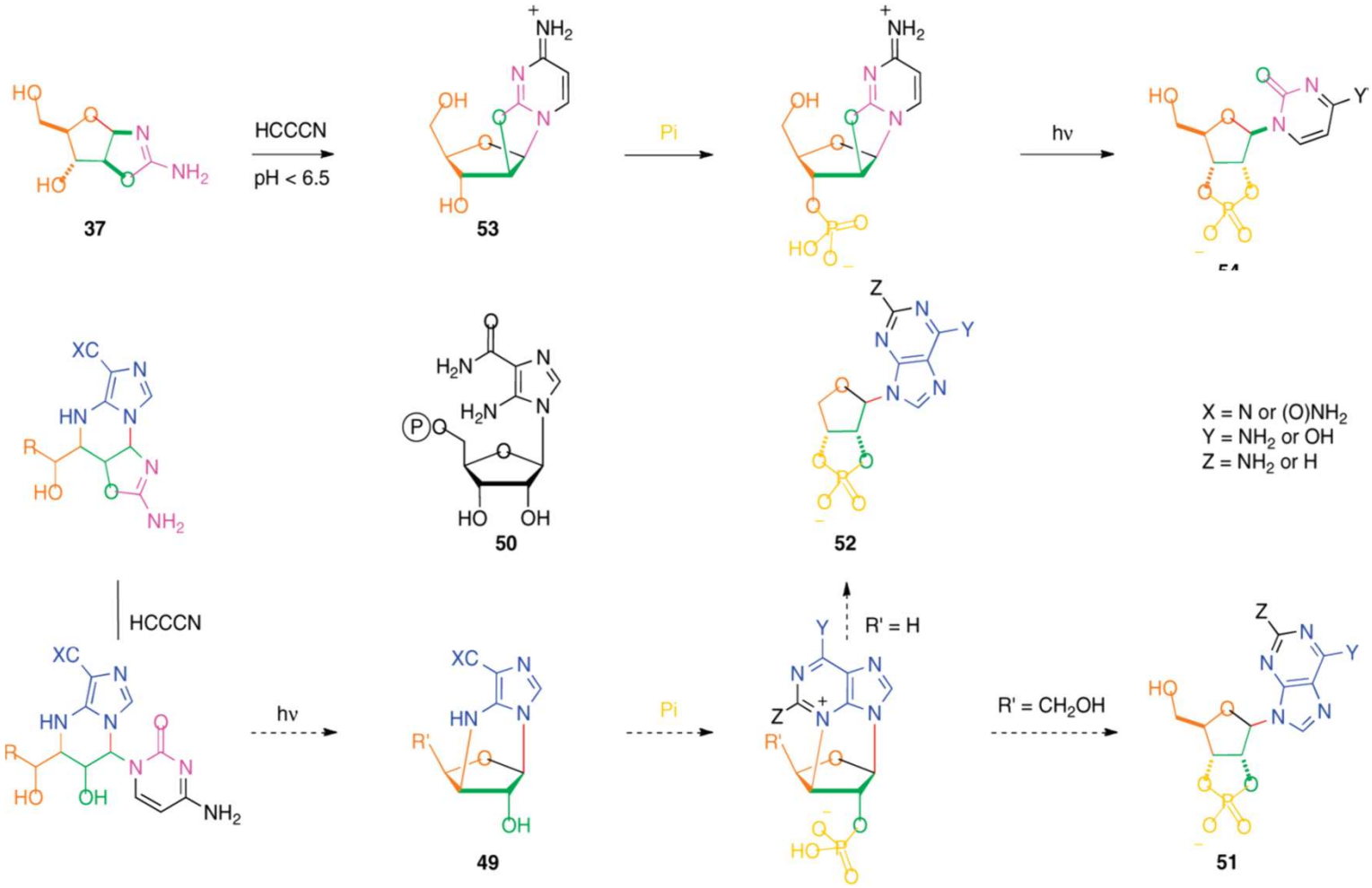

M. W. Powner, J. D. Sutherland, J. W. Szostak *J. Am. Chem. Soc.* **2010**, *132*, 16677-16688

Prebiotic synthesis of deoxyribonucleosides

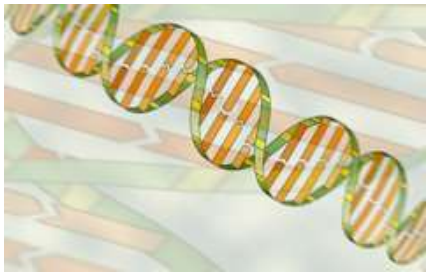

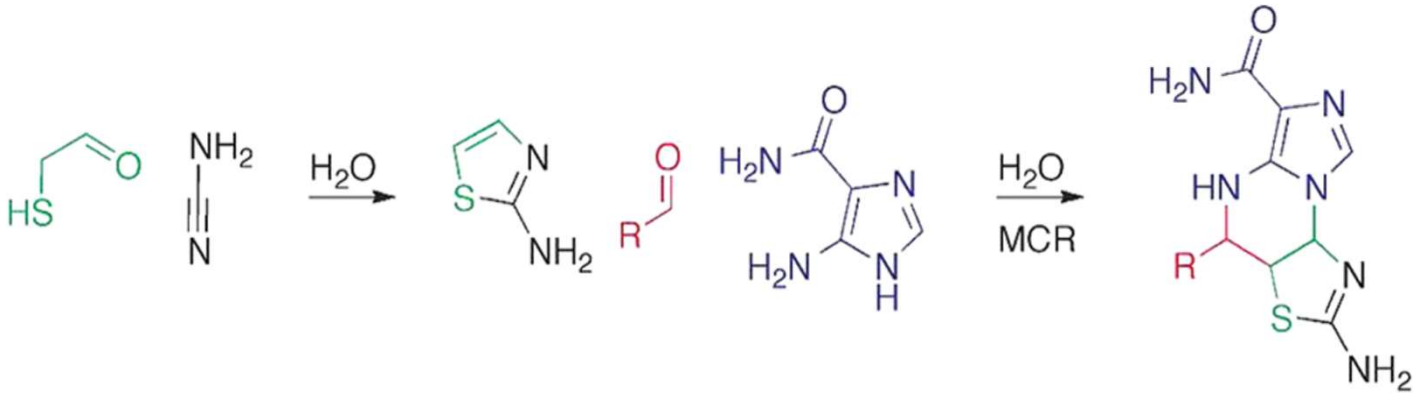

proposed multicomponent deoxyribonucleotide syntheses

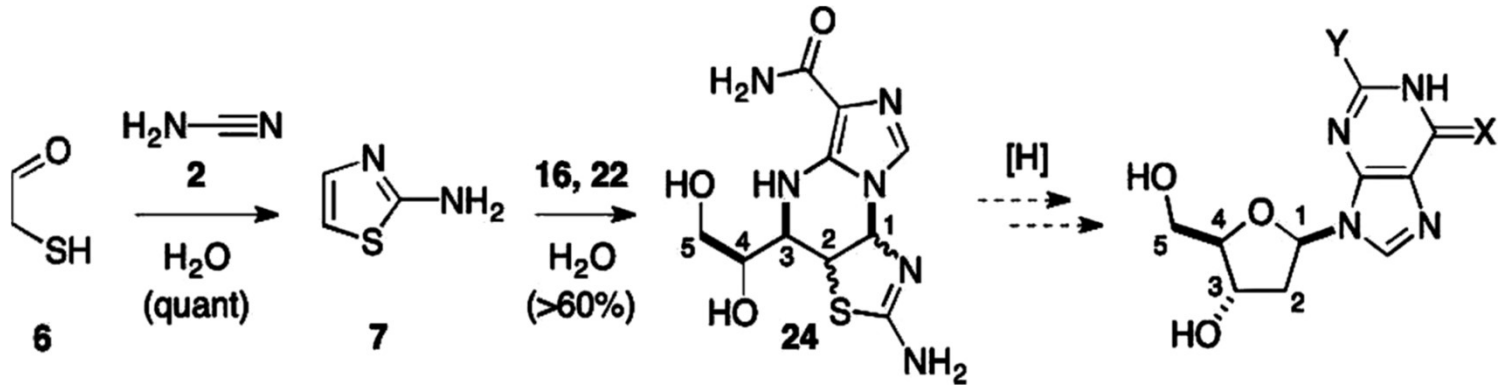

M. W. Powner, S.-L. Zheng, J. W. Szostak *J. Am. Chem. Soc.* **2012**, *134*, 13889-13895

Purine nucleoside synthesis - alternatives

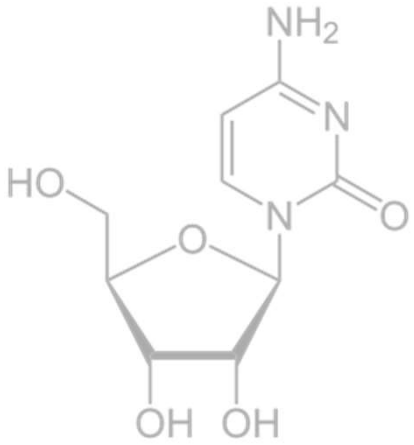

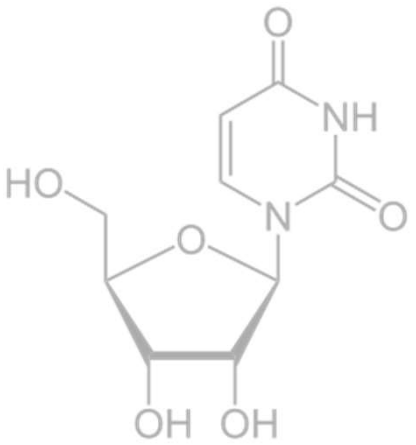

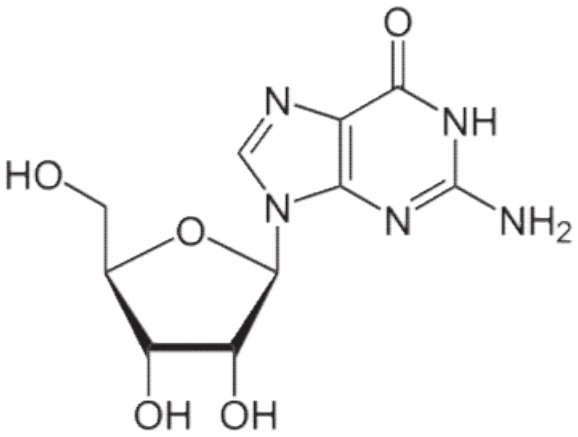

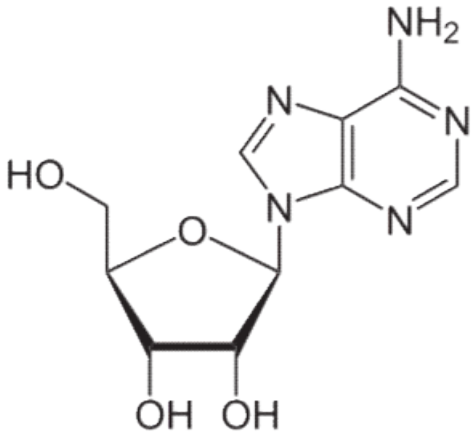

Prebiotic synthesis of purine nucleosides –FaPY pathway

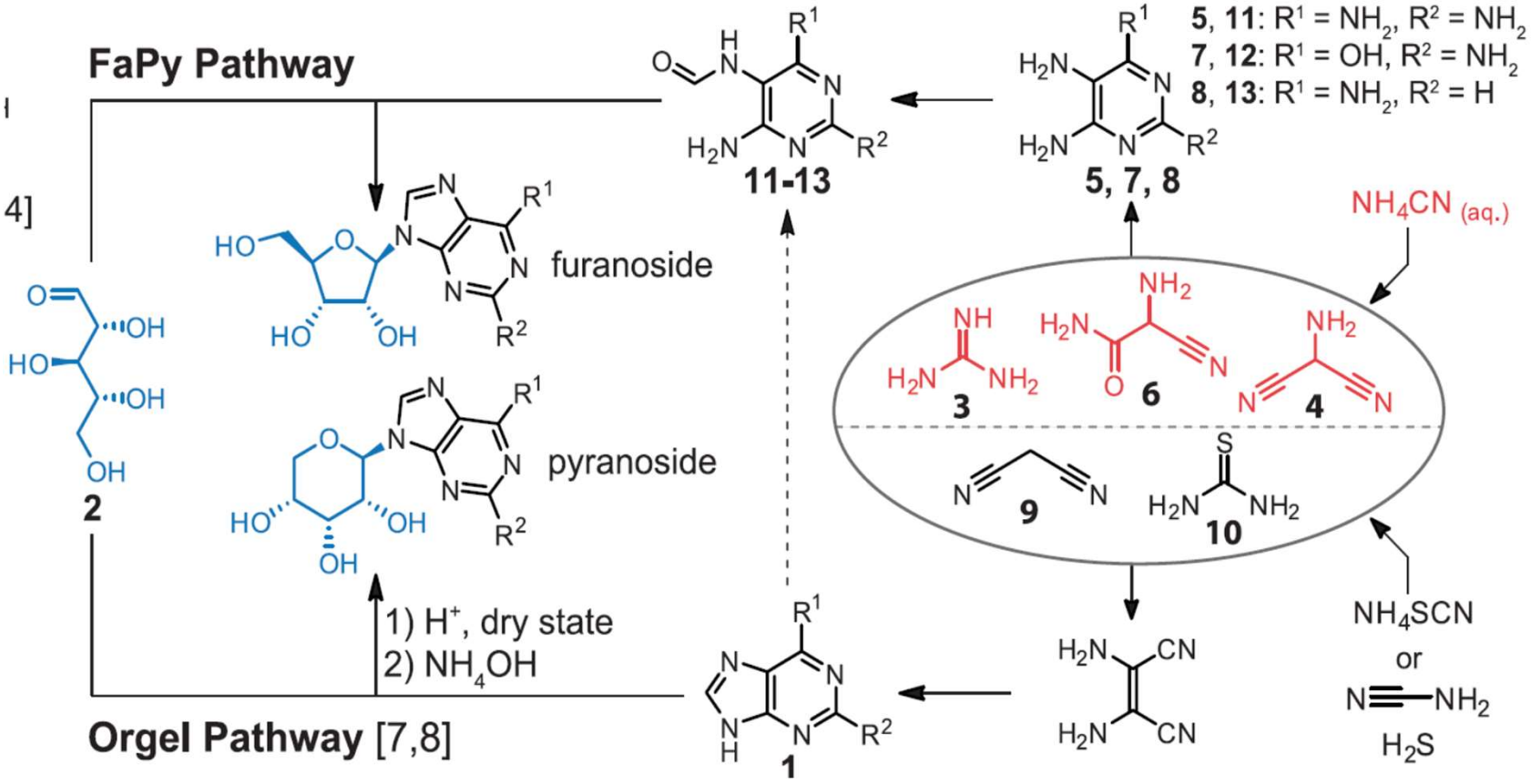

T. Carell, *Nature* **2016**, *352(6287)*, 833-836

Prebiotic syntheses of aminopyrimidines

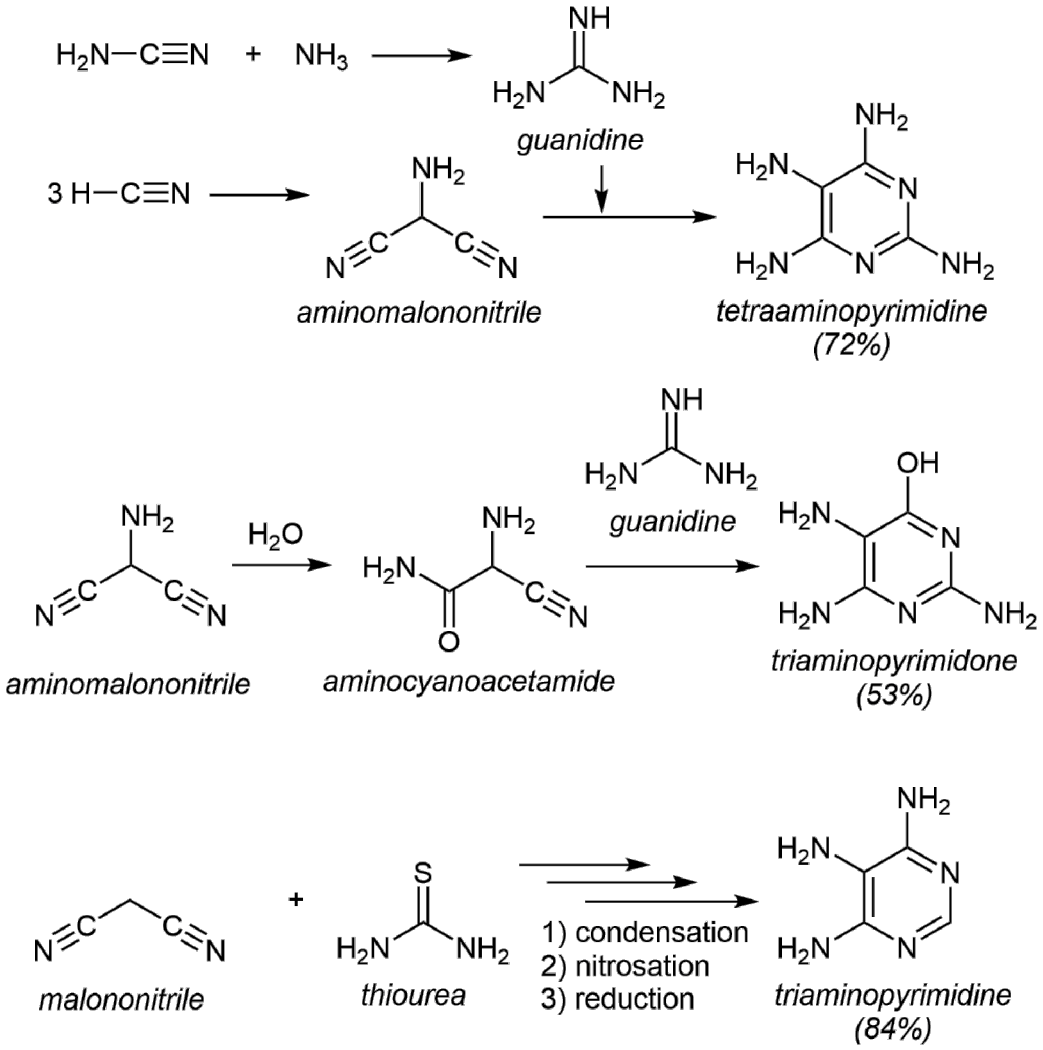

T. Carell, *Nature* **2016**, *352(6287)*, 833-836

Prebiotic synthesis of purine nucleosides –FaPY pathway

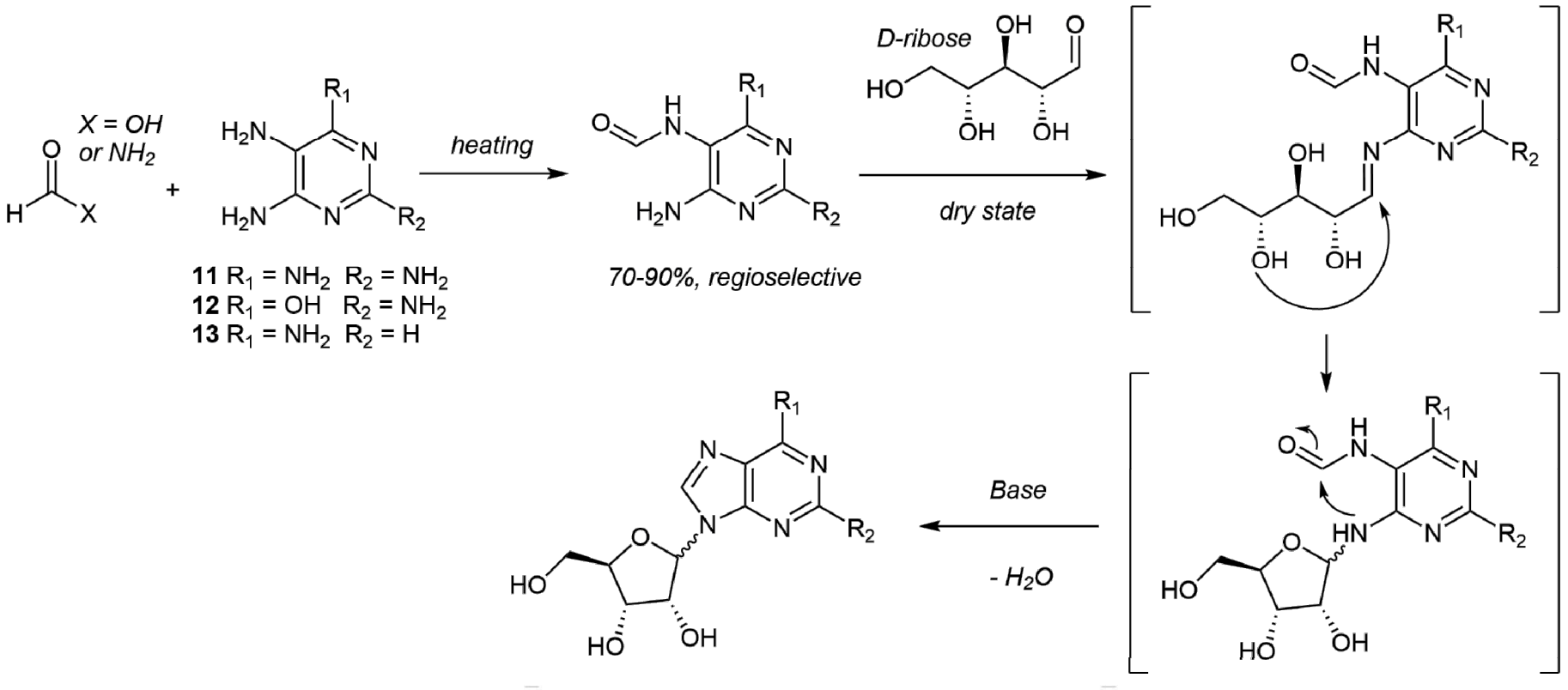

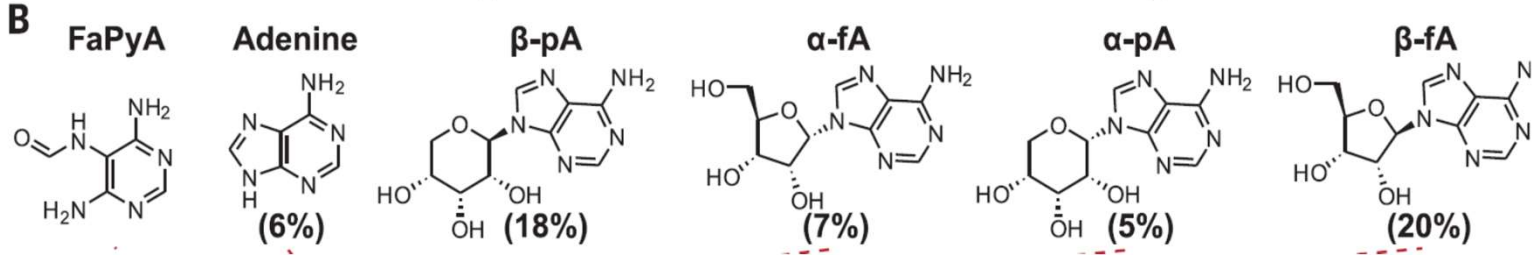

T. Carell, *Nature* **2016**, *352(6287)*, 833-836

Prebiotic synthesis of purine nucleosides –FaPY pathway

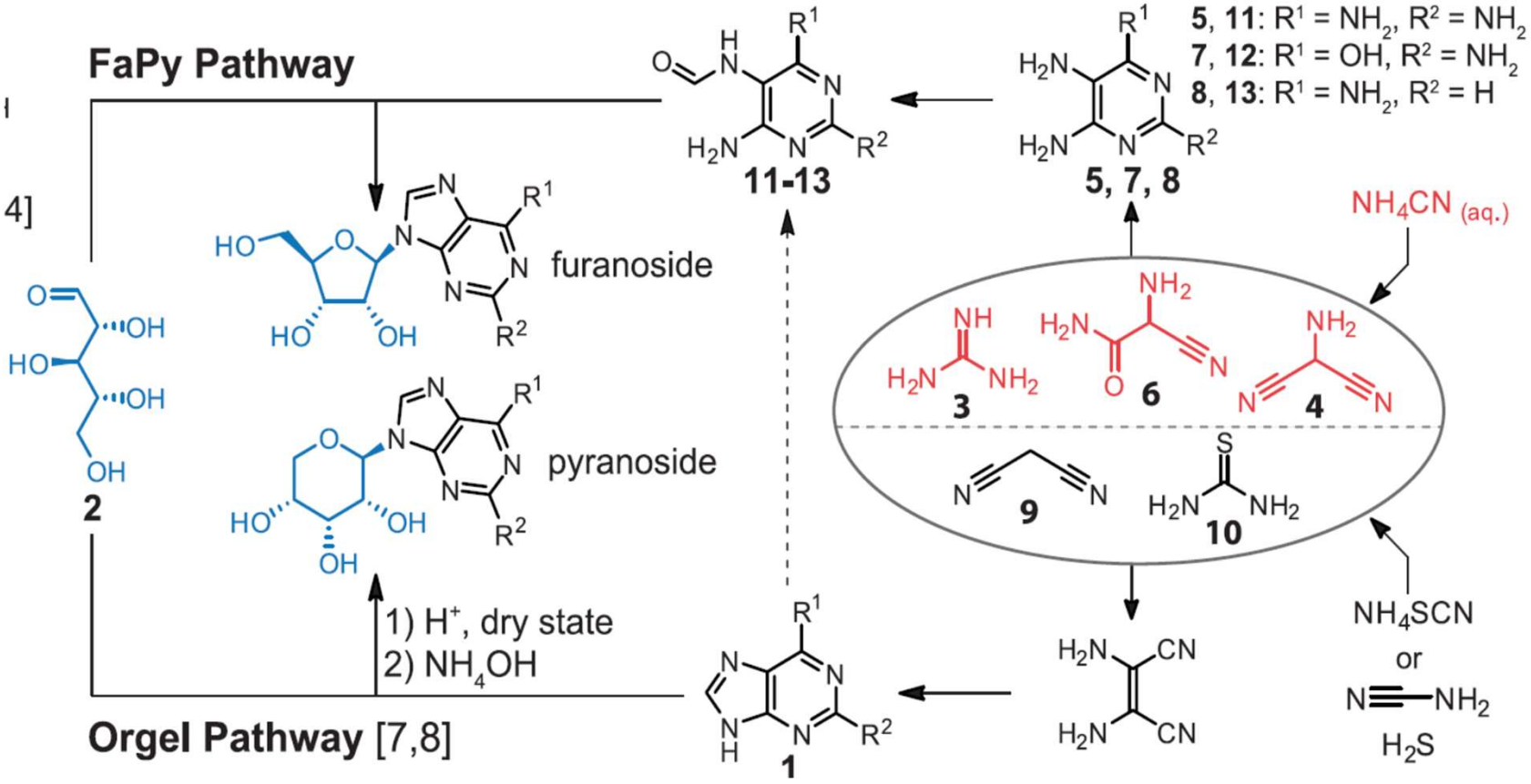

T. Carell, *Nature* **2016**, *352(6287)*, 833-836

Unified prebiotic synthesis of pyrimidine and purine ribonucleotides

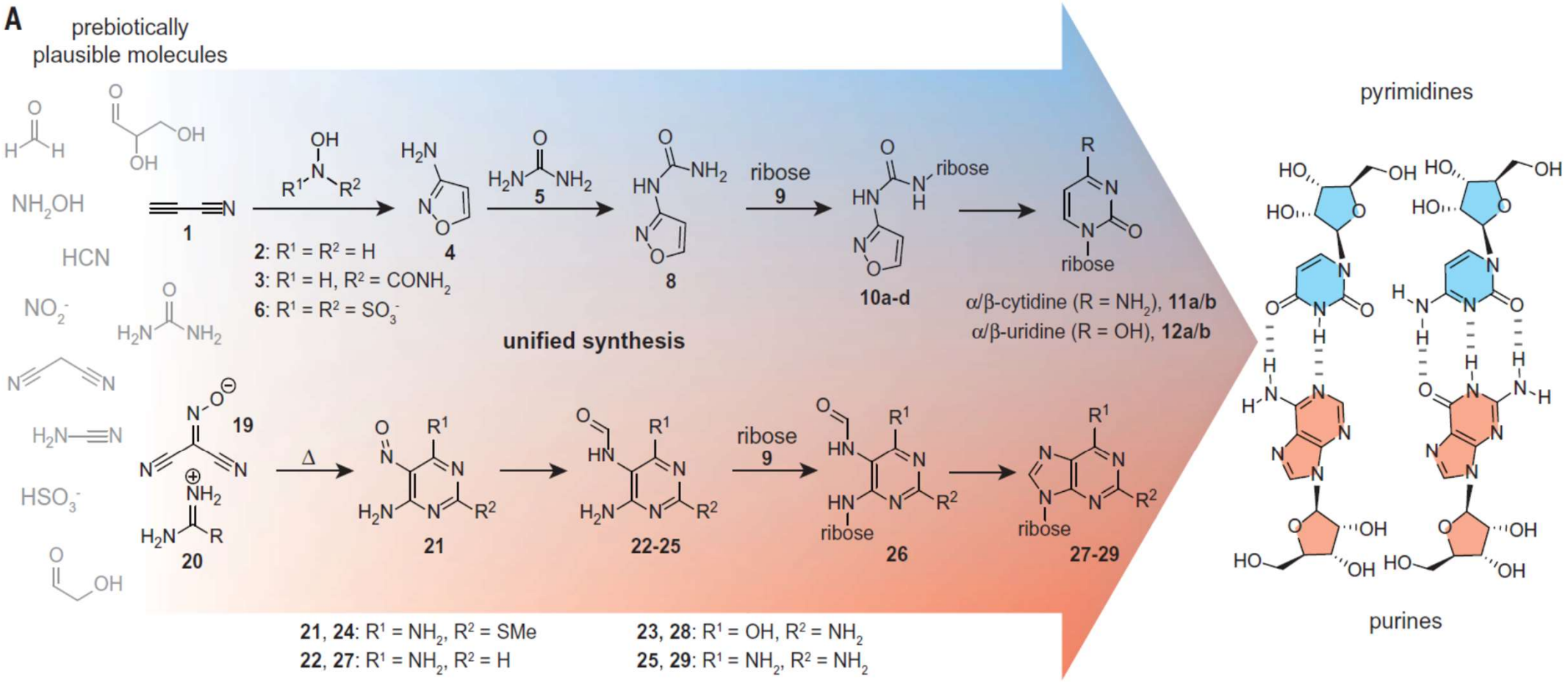

S. Becker, J. Feldmann, S. Wiedemann, ..., T. Carell, *Science* **2019**, *366*, 76-82

Unified prebiotic synthesis of pyrimidine and purine ribonucleotides

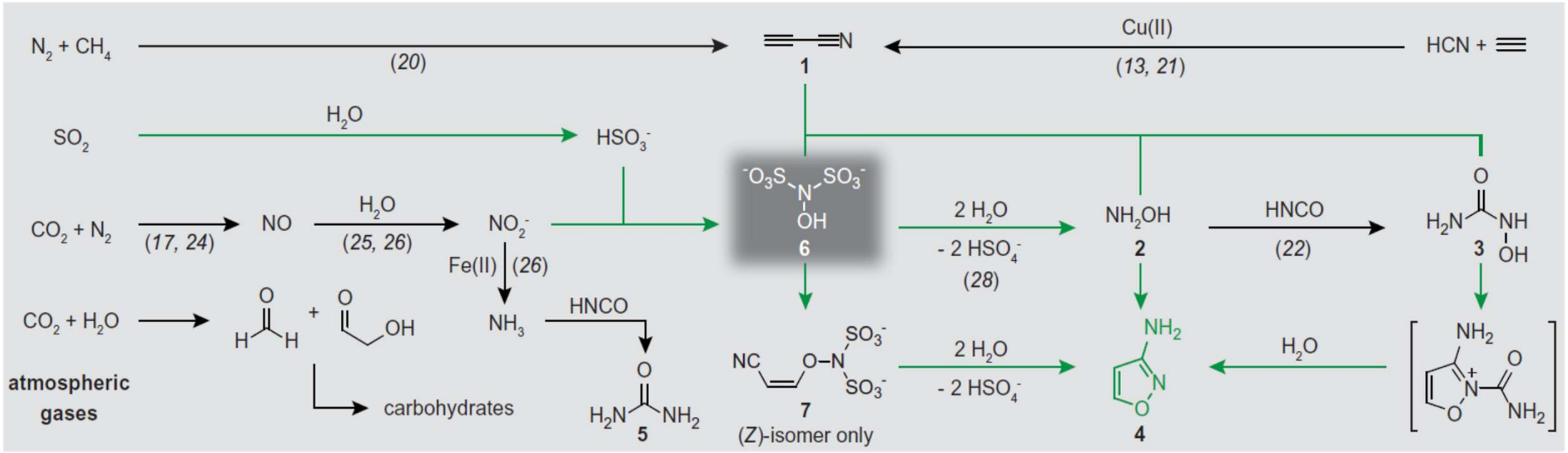

S. Becker, J. Feldmann, S. Wiedemann, ..., T. Carell, *Science* **2019**, *366*, 76-82

Unified prebiotic synthesis of pyrimidine and purine ribonucleotides

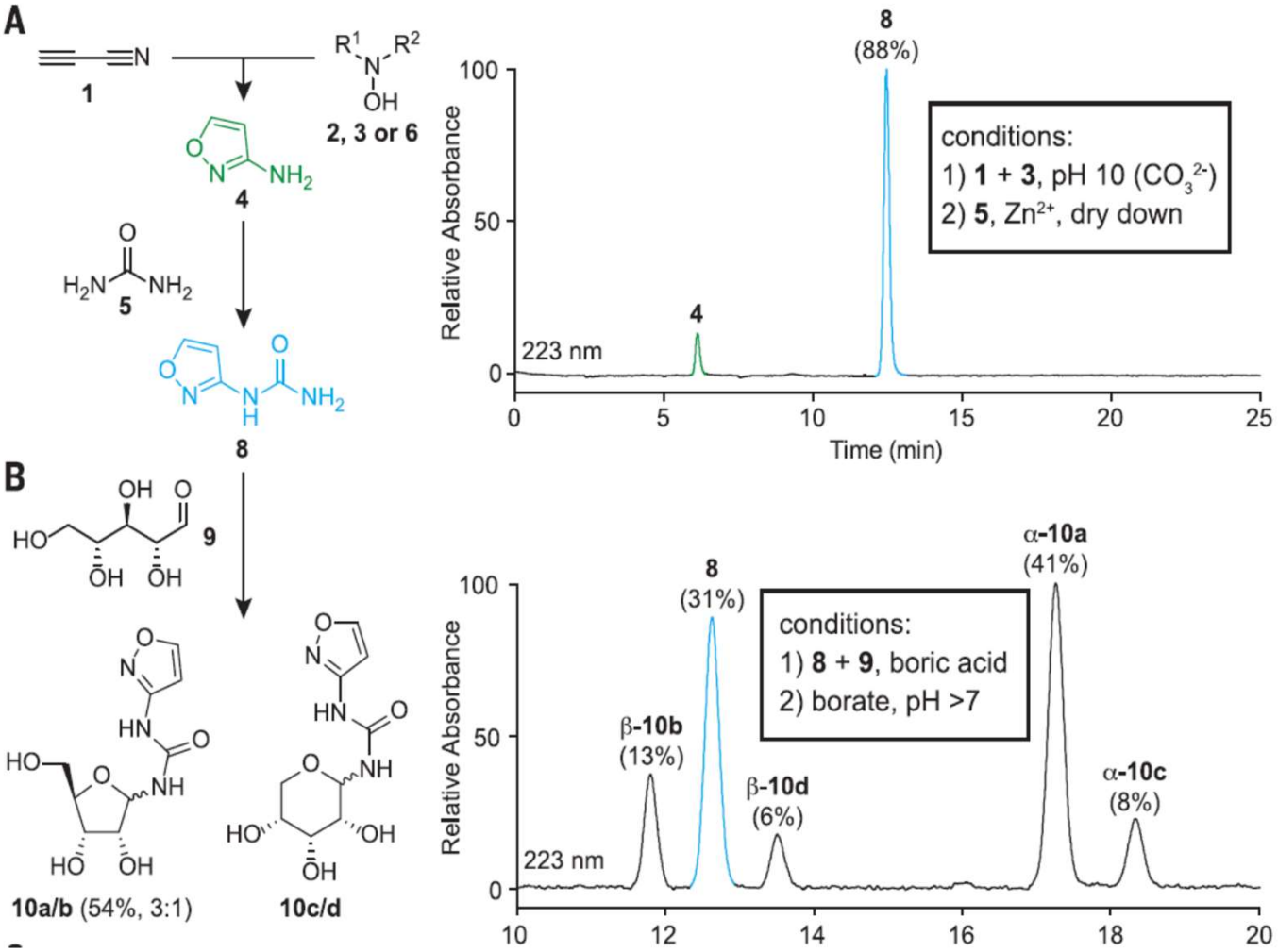

S. Becker, J. Feldmann, S. Wiedemann, ..., T. Carell, *Science* **2019**, *366*, 76-82

Unified prebiotic synthesis of pyrimidine and purine ribonucleotides

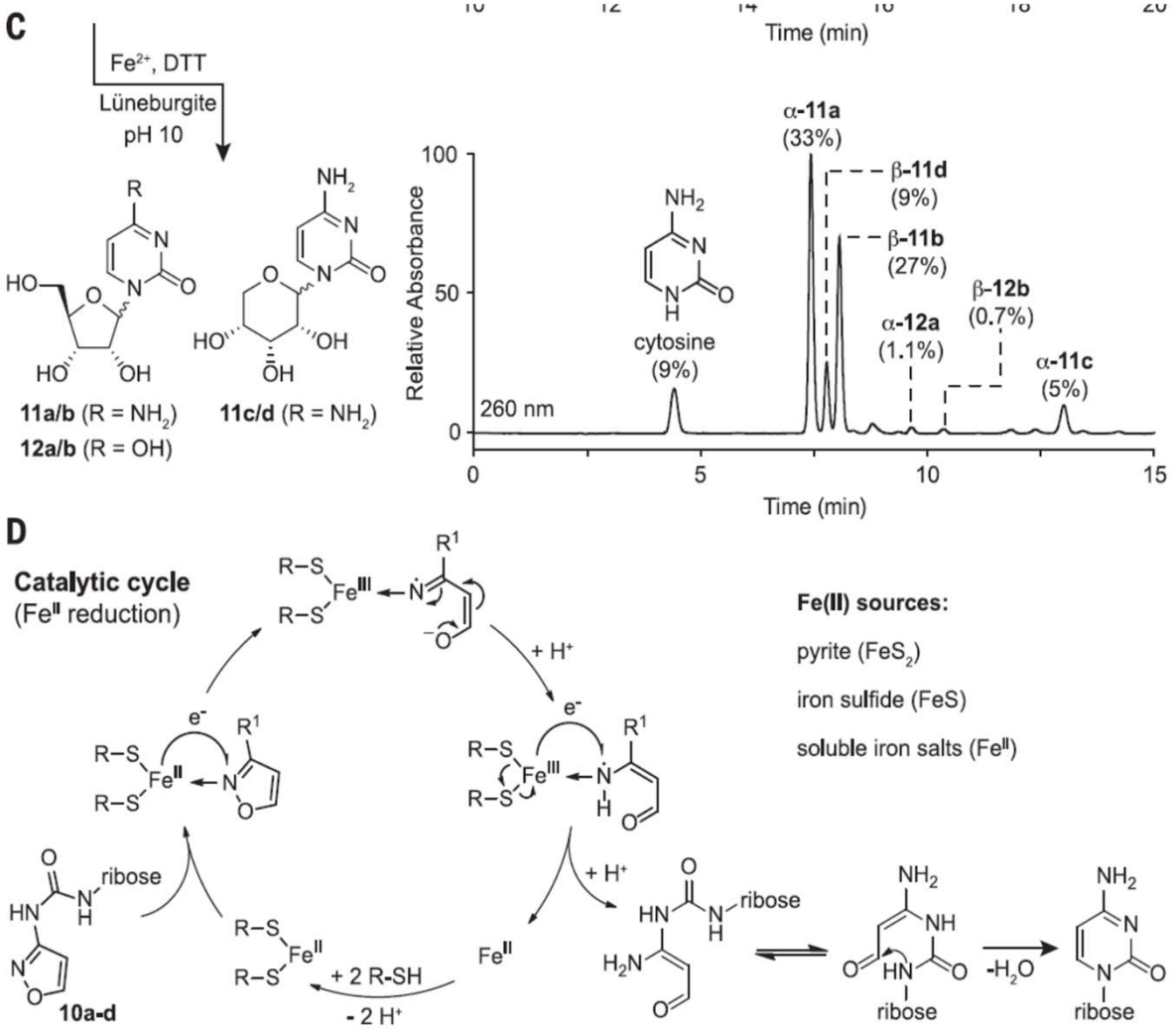

S. Becker, J. Feldmann, S. Wiedemann, ..., T. Carell, *Science* **2019**, *366*, 76-82

Unified prebiotic synthesis of pyrimidine and purine ribonucleotides

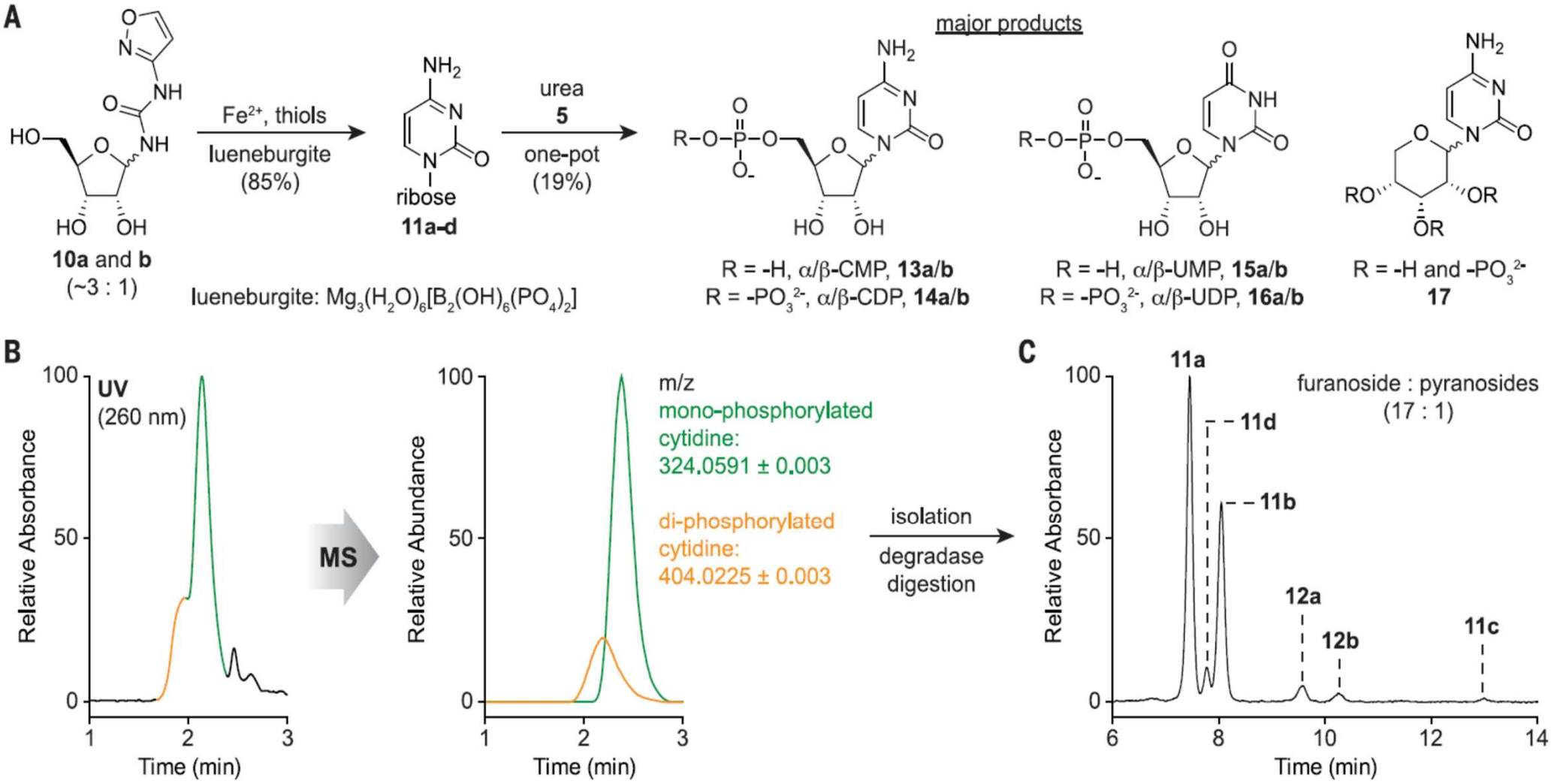

S. Becker, J. Feldmann, S. Wiedemann, ..., T. Carell, *Science* **2019**, *366*, 76-82

Unified prebiotic synthesis of pyrimidine and purine ribonucleotides

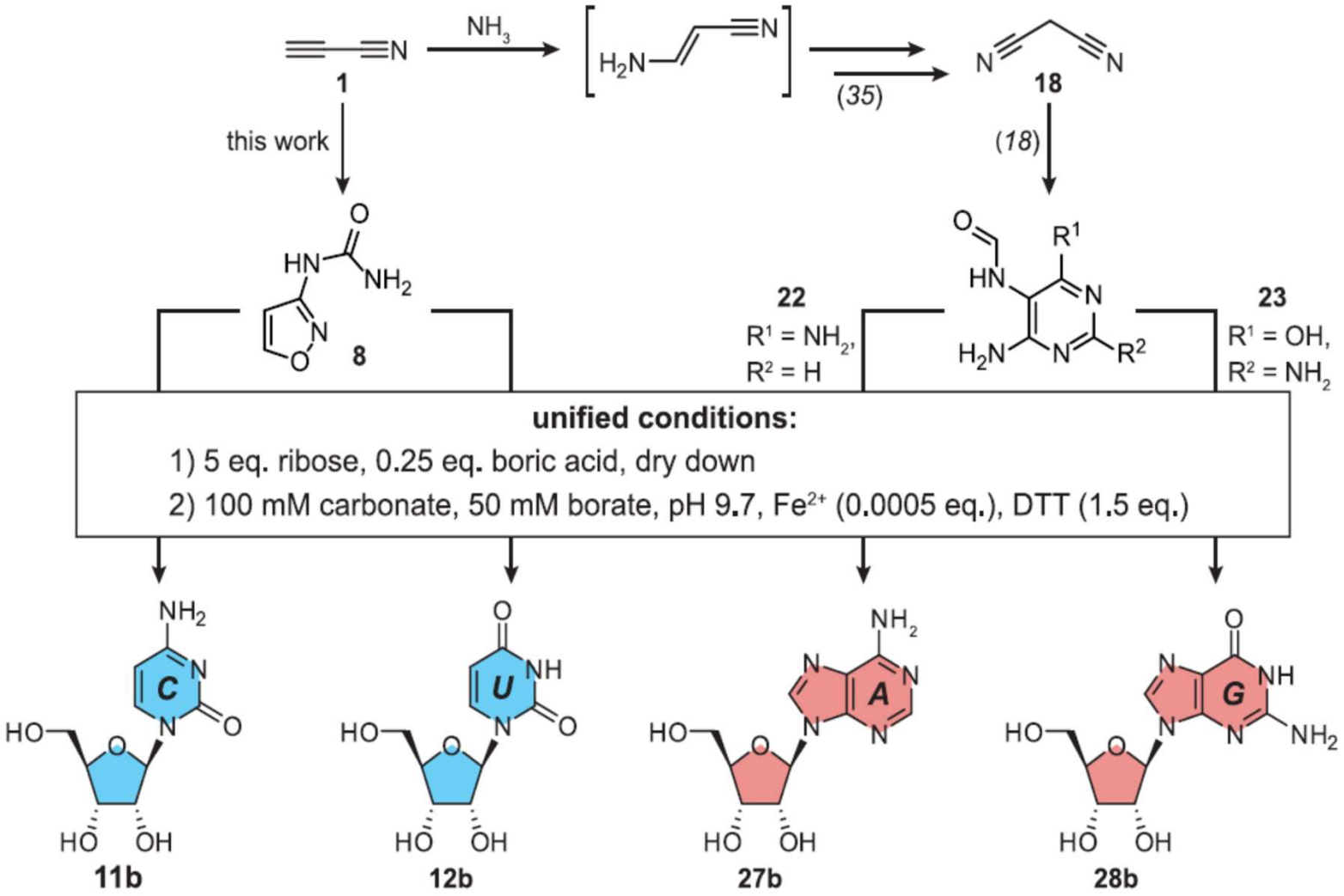

S. Becker, J. Feldmann, S. Wiedemann, ..., T. Carell, *Science* **2019**, *366*, 76-82

Unified prebiotic synthesis of pyrimidine and purine ribonucleotides

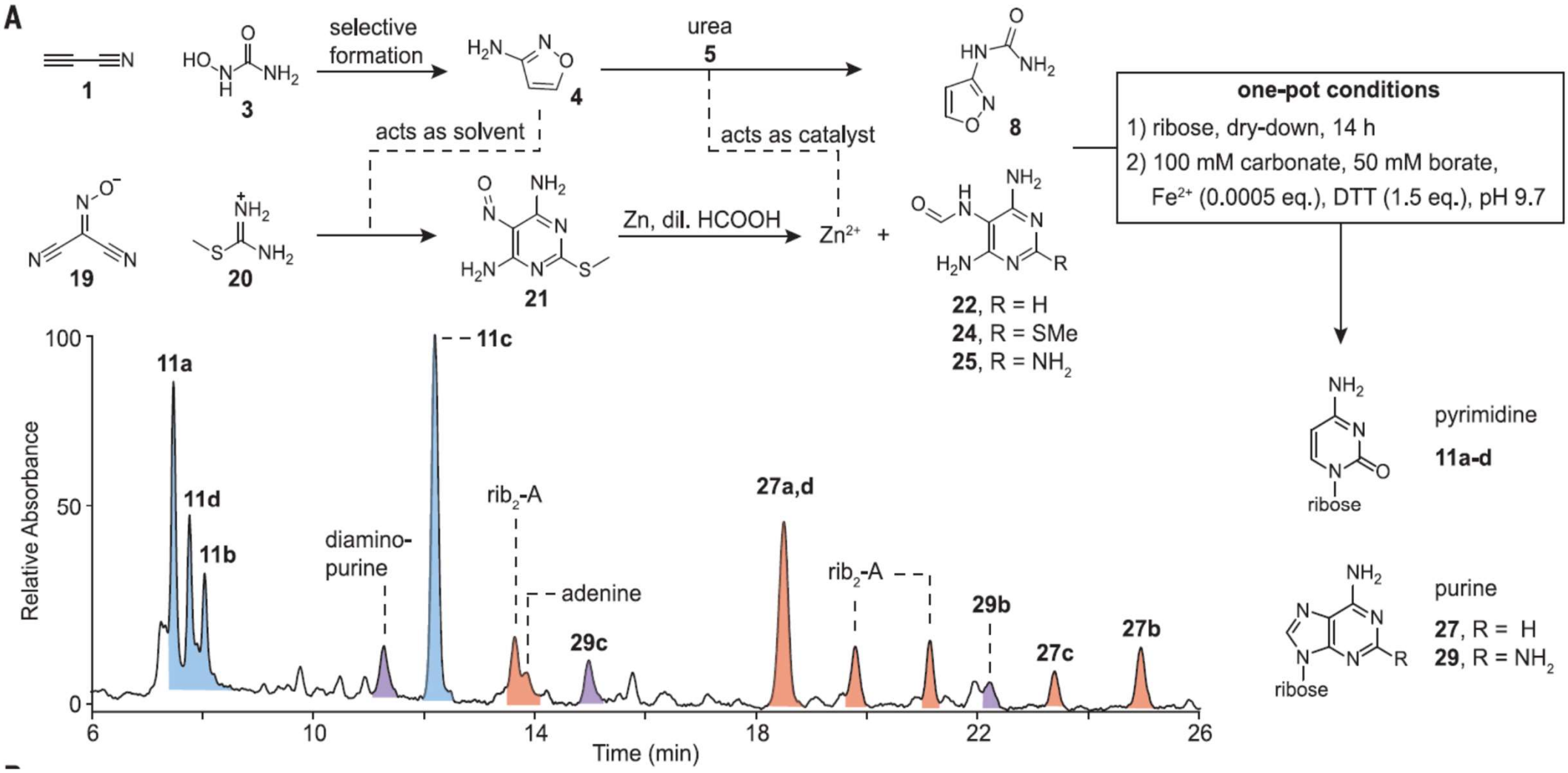

S. Becker, J. Feldmann, S. Wiedemann, ..., T. Carell, *Science* **2019**, *366*, 76-82

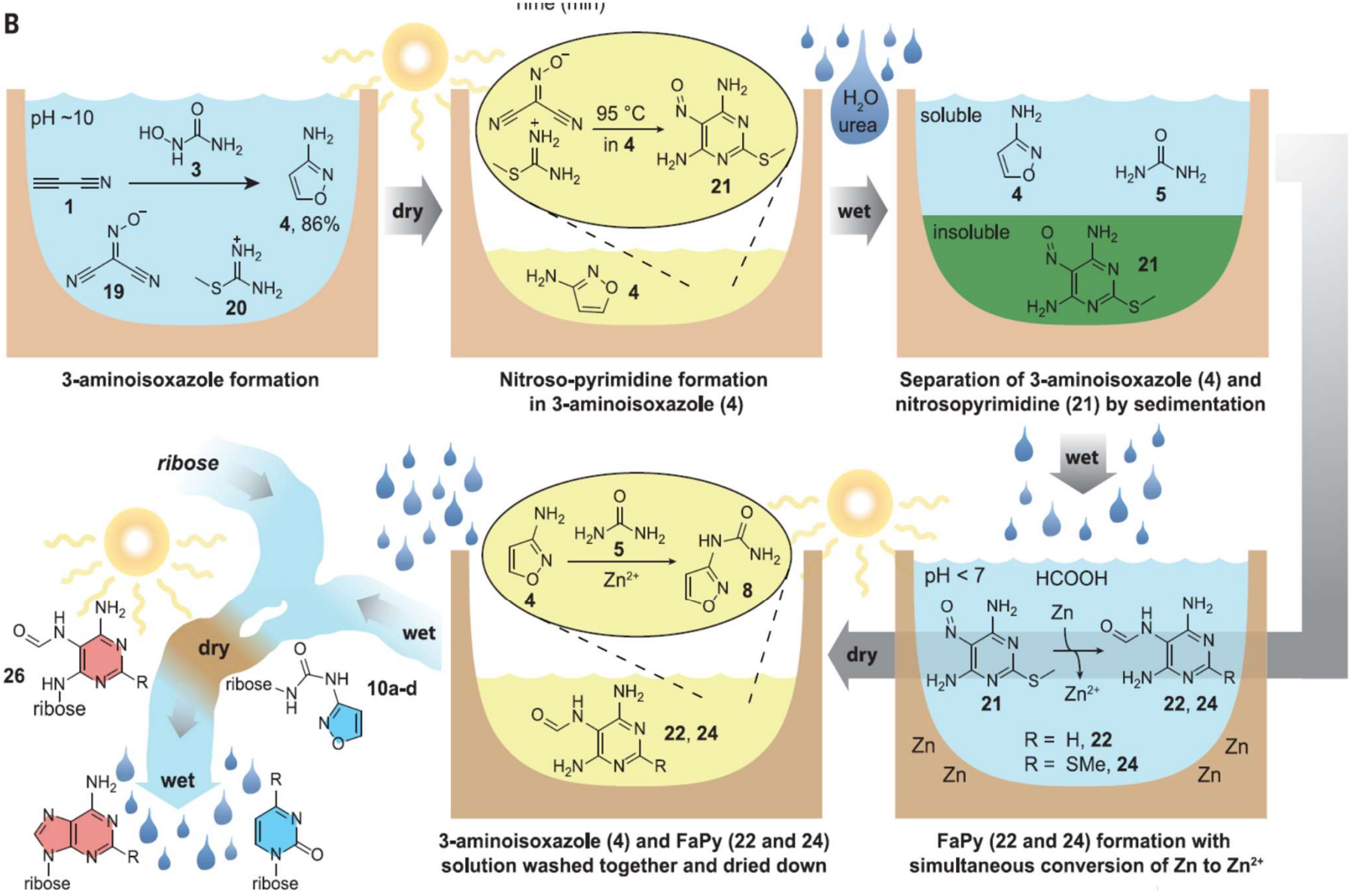

S. Becker, J. Feldmann, S. Wiedemann, ..., T. Carell, *Science* **2019**, *366*, 76-82

Prebiotic phosphorylations and the origins of protometabolism

Selective Phosphorylation of Glycolaldehyde and Aldol Reactions of Glycolaldehyde Phosphate

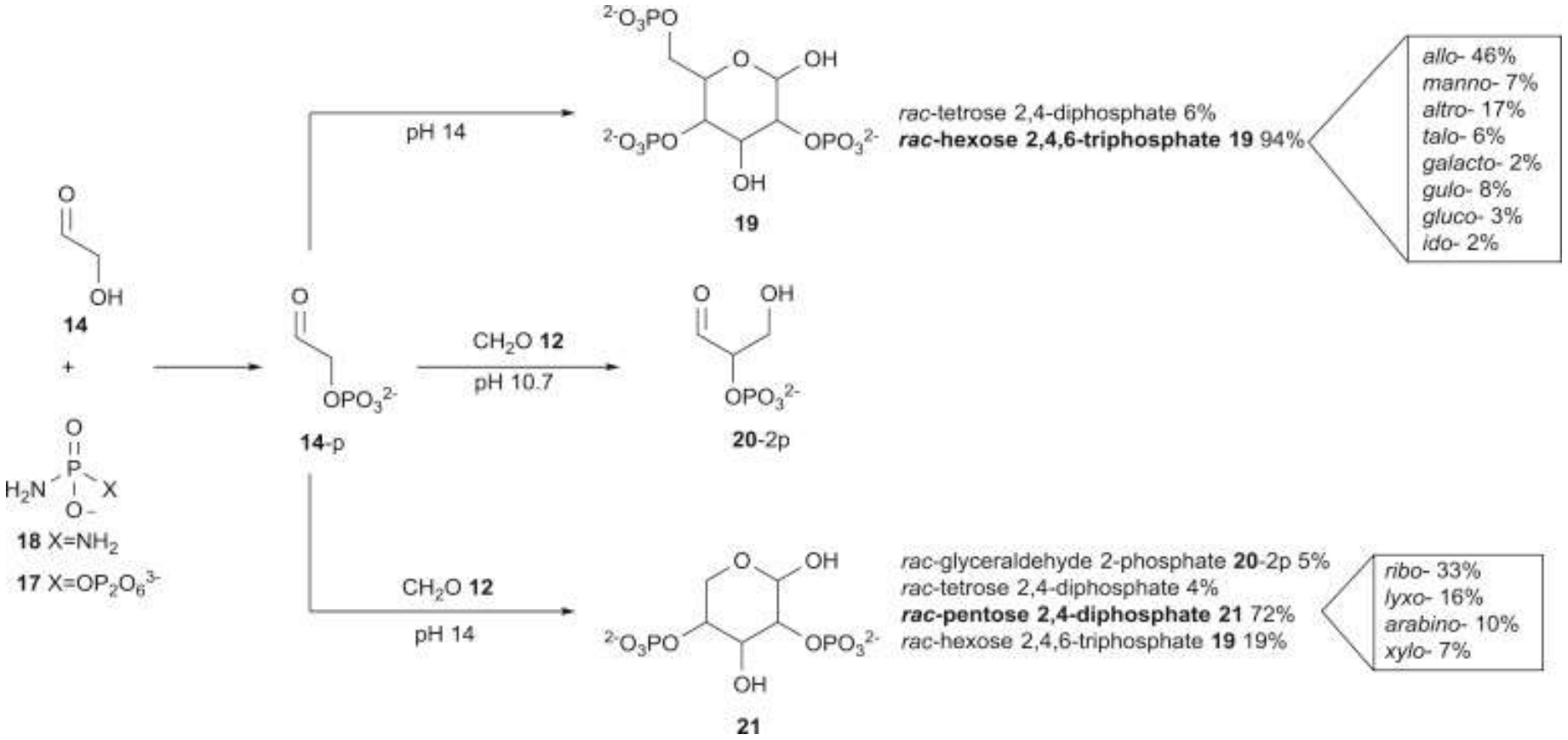

S. Islam, M. W. Powner *Chem* **2017**, *2*, 470-501

Prebiotic Reconstruction of the Triose Glycolysis Pathway by Selective α-Phosphorylation of Sugars

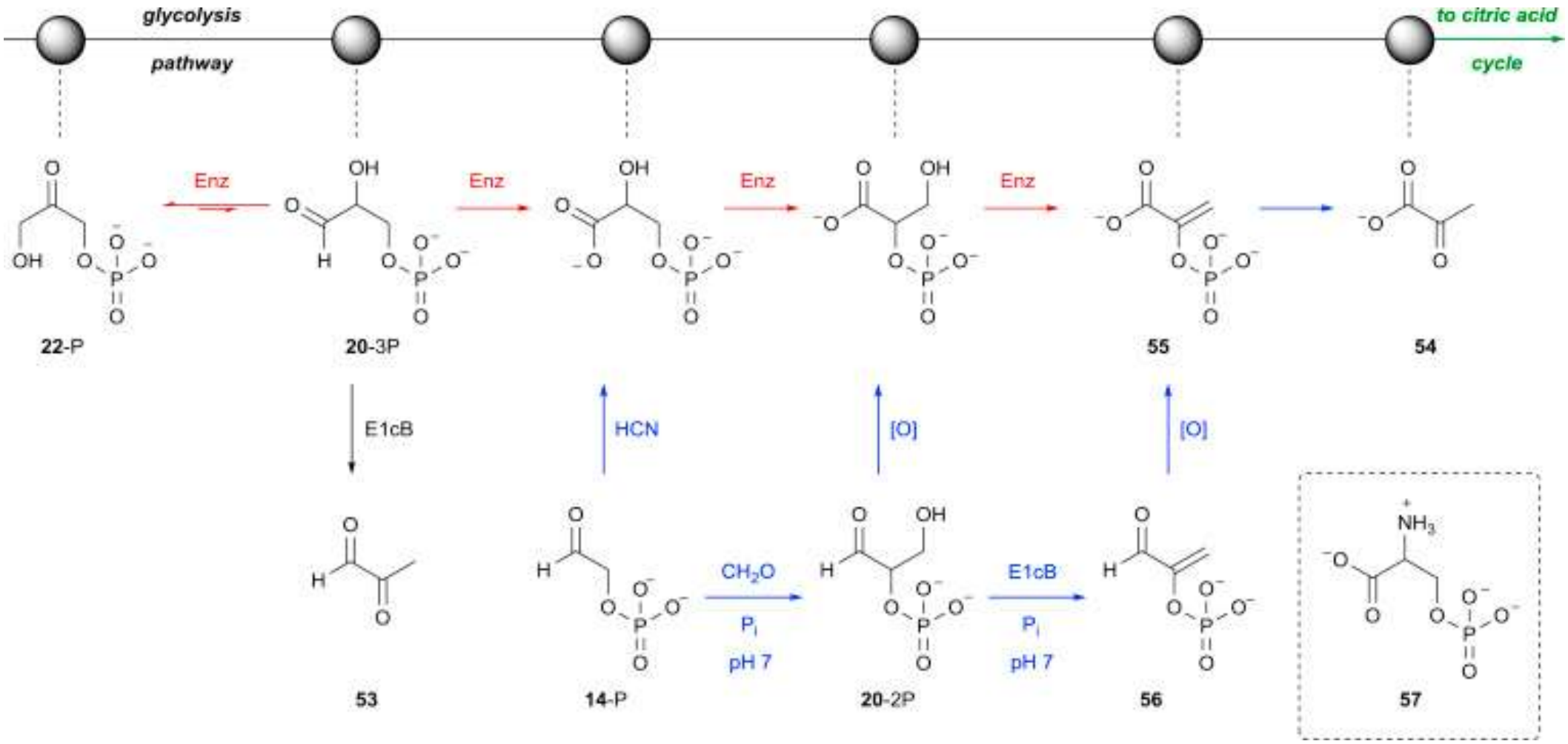

S. Islam, M. W. Powner *Chem* **2017**, *2*, 470-501

Prebiotic soup - summary

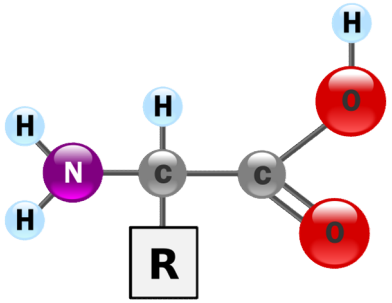

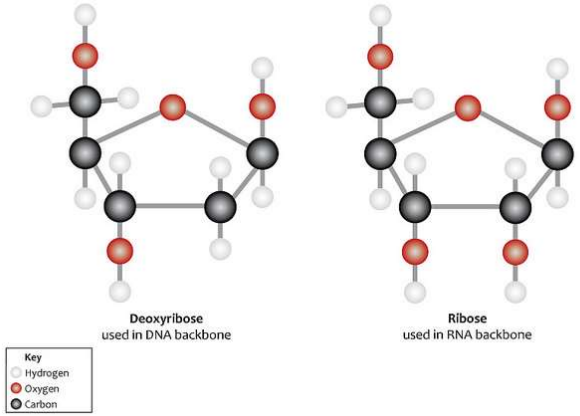

vivianite